Paleohydrology of the Lower Colorado River Basin and Implications for Water Supply Availability

Jeffrey J. Lukas
Lisa Wade
Balaji Rajagopalan

October 2012

Completion Report No. 223

Colorado State University

Acknowledgements

Funding for this project was provided by the Colorado Water Institute, the Colorado River District, the CU-CIRES Western Water Assessment program (itself supported by the NOAA Climate Program Office), and the CU Department of Civil and Environmental Engineering (graduate student support for Lisa Wade).

Connie Woodhouse and David Meko of the University of Arizona generated several of the tree-ring reconstructions of streamflow described in this report (see Table 1 and related text), and also provided nearly all of the underlying tree-ring data used for this project, having collected them for previous studies.

David Kanzer and Eric Kuhn of the Colorado River District provided technical guidance throughout the project, and also provided the basemap for the Colorado River basin shown in Figure 1.

Subhrendu Gangopadhyay and Tom Pruitt of the U.S. Bureau of Reclamation provided the VIC hydrology model output that was used in comparisons with the naturalized streamflow records.

Eric Kuhn of the Colorado River District provided the initial and continuing encouragement for this project.

This report was financed in part by the U.S. Department of the Interior, Geological Survey, through the Colorado Water Institute. The views and conclusions contained in this document are those of the authors and should not be interpreted as necessarily representing the official policies, either expressed or implied, of the U.S. Government.

Additional copies of this report can be obtained from the Colorado Water Institute, E102 Engineering Building, Colorado State University, Fort Collins, CO 80523-1033 970-491-6308 or email: cwi@colostate.edu, or downloaded as a PDF file from http://www.cwi.colostate.edu.

Colorado State University is an equal opportunity/affirmative action employer and complies with all federal and Colorado laws, regulations, and executive orders regarding affirmative action requirements in all programs. The Office of Equal Opportunity and Diversity is located in 101 Student Services. To assist Colorado State University in meeting its affirmative action responsibilities, ethnic minorities, women and other protected class members are encouraged to apply and to so identify themselves.

Paleohydrology of the Lower Colorado River Basin and implications for water supply availability

Jeffrey J. Lukas
Lisa Wade*
Balaji Rajagopalan

University of Colorado, Boulder

Completion Report to the Colorado Water Institute

October 2012

*Current affiliation: Riverside Technology, Inc., Fort Collins, CO

Table of Contents

Abstract **1**

1. Background and Justification **2**

2. Methods and Results **3**

2.1 Tree-ring reconstructions – background and previous work **4**

2.2 Development of naturalized observed flow records **5**

2.2.1 Gila River *5*

2.2.2 Mainstem Lower Colorado River *6*

2.3 Compilation of tree-ring chronologies **8**

2.4 Generation of tree-ring reconstructions **9**

2.4.1 Overview of methods *9*

2.4.2 LOWESS multiple regression *11*

2.4.3 K-NN non-parametric *11*

2.4.4 Local Poly – PCAreg *11*

2.4.5 Extreme Value Analysis (EVA) *12*

2.5 Intermediate modeling steps **13**

2.5.1 Local Poly – PCAreg *13*

2.5.2 Extreme Value Analysis (EVA) *13*

2.6 Results – tree-ring reconstructions **14**

2.6.1 Gila River – naturalized flows *14*

2.6.2 Gila River – gaged flows *19*

2.6.3 Mainstem intervening flows – naturalized flows *20*

2.6.4 Summary *21*

2.7 System response analysis **22**

2.7.1 Background *22*

2.7.2 Methods *23*

2.7.3 Results *26*

3. Conclusions **30**

4. References **32**

List of Tables

Table 1. Matrix showing the observed streamflow time-series (columns) that were reconstructed with one or more of the statistical approaches (rows).....10

Table 2. The four management alternatives (A–D) considered in the system response modeling, and the demand schedule and delivery shortage policy used for each.....25

Table 3. The cuts to LCRB deliveries mandated at specified reservoir levels under the Interim Guidelines (left) and the Aggressive Shortage Policy (right).....26

List of Figures

Figure 1. Colorado River Basin (CRB). The basin is divided at Lee(s) Ferry (red dot) for legal and management purposes into an UCRB and LCRB (red boundaries). The watershed of the Gila River is outlined in black, with the Gila near Dome, AZ gage shown in green. USBR's nine CRSS model nodes in the LCRB are shown as blue and yellow dots. The intervening flows at the five blue nodes are well correlated with precipitation while the four yellow nodes are not. We used only the five blue nodes to calibrate the Lower Colorado mainstem flow reconstruction. See further details in the text.....2

Figure 2. Schematic showing the development of the streamflow reconstructions (dark blue) and their subsequent use as one of the inputs into the system response analysis (light blue).....4

Figure 3. Gaged annual streamflows (1929–2011; USGS) for the Gila River at two gages: Safford Valley, near Solomon, AZ, in the headwaters of the basin (red); and near Dome, AZ, at the confluence of the Gila and the Colorado River (blue). The flows at Safford represent near-natural conditions; intensive use of the river downstream of Safford has resulted in flows at the mouth that are near-zero in most years, spiked with periodic very large flows, such as in 1980 and 1993.....5

Figure 4. Our model (blue) of estimated natural annual streamflows (1915–2010) for the Gila River near Dome, AZ, at the confluence of the Gila and the Colorado River. The model predictors are gaged headwaters flows, including the Safford gage shown in Figure 2, calibrated on natural flows for 1897–1943 estimated in Reclamation (1946) (dashed black line).....6

Figure 5. The natural flows for the nine nodes of the CRSS model in the Lower Colorado Basin fell into two groups: five good nodes whose flows are well-correlated with observed hydroclimate in the basin, and four noise nodes, whose flows are not.....7

Figure 6. The locations of the 61 tree-ring site chronologies whose data were compiled for this study (green triangles).....8

Figure 7. The results of the k-means cluster analysis on the 35 screened chronologies. Three clusters (colored ovals) were discerned, with two of them producing spatially contiguous groupings.....13

Figure 8. The Local Poly reconstruction model (blue) compared with the observed (naturalized) Gila River flows (black) over the calibration period of 1915–2005. The gray band is the confidence interval around the reconstructed values. This model captures the low flows extremely well, but tends to underestimate the high flows, particularly in 1993.....14

Figure 9. Five different reconstruction models, compared with the observed (naturalized) Gila River flows over the calibration period of 1915-2005. (Method 1 is the Local Poly method.) All of the models capture the low flows better than the high flows, which are consistently underestimated.....15

Figure 10. The Local Poly reconstruction of Gila River flows (blue), compared with the observed (naturalized) Gila River flows (black) over the period of 1612–2005. Note that the model generates high flows even higher than the 1993 observed flow.....16

Figure 11. Five different reconstructions of annual Gila River flow, over the period of 1612–2005. (Method 1 is the Local Poly method.) The reconstructed variability is very similar among the reconstructions, with the reconstructed magnitudes differing most in the high-flow years.....16

Figure 12. Five different reconstructions of annual Gila River flow, smoothed with five-year running averages, over the period of 1612–2005. (Method 1 is the Local Poly method.) The timing and magnitude of decadal-scale high- and low-flow periods is very similar, with the notable exception of the magnitude of the very high-flow period around 1750.....17

Figure 13. Combined three-method reconstruction of annual Gila River flow (see text) over the period of 1612–2005. The annual values are shown with the thin line, and the five-year running means with the thick line.....17

Figure 14. The Extreme Value Analysis Peaks-over-Threshold model compared to the observed (naturalized) Gila River flows over the calibration period of 1915–2005. The blue line is the reconstructed flow magnitudes (left-hand y-axis) and the purple crosses are the reconstructed probability of exceeding the threshold of two MAF.....18

Figure 15. The Extreme Value Analysis Peaks-over-Threshold reconstruction of naturalized Gila River flows over the reconstructed period of 1612–2005. The blue line is the reconstructed flow magnitudes (left-hand y-axis) and the purple crosses are the reconstructed probability of exceeding the threshold of two MAF.....18

Figure 16. The Extreme Value Analysis Peaks-over-Threshold model compared to the observed (gaged) Gila River flows over the calibration period of 1930–2005. The blue line is the reconstructed flow magnitudes (left-hand y-axis) and the purple crosses are the reconstructed probability of exceeding the selected threshold of 0.2 MAF.....19

Figure 17. The Extreme Value Analysis Peaks-over-Threshold reconstruction of gaged Gila River flows over the reconstructed period of 1612–2005. The blue line is the reconstructed flow magnitudes (left-hand y-axis) and the purple crosses are the reconstructed probability of exceeding the threshold of 0.2 MAF.....20

Figure 18. Three different reconstruction models, compared with the observed five-good-node LCRB (non-Gila) flows over the calibration period of 1906–2005. (Method 1 is the Local Poly method.) As with the Gila River, all of the models capture the low flows better than the high flows, which are consistently underestimated.....21

Figure 19. Three different reconstructions of annual five-good-node LCRB (non-Gila) flow, over the period of 1612–2005. (Method 1 is the Local Poly method.) The reconstructed variability is less similar among the reconstructions than with the Gila reconstructions.....21

Figure 20. Schematic of the water-balance model used for the system response analysis, modified from Rajagopalan et al. (2009) to include the Gila River inflows. The “bathtub” represents the aggregate CRB reservoir storage capacity of 60 MAF.....24

Figure 21: Risk of drying (depleting all reservoir storage in a given year) for Alternatives A and B. Including the Gila River into the water-balance model decreases the risk of drying for all climate change scenarios. (left) No climate change induced flow reductions. (center) 10 percent climate change induced flow reduction by 2057. (right) 20 percent climate change induced flow reduction by 2057.....27

Figure 22: Risk of drying (depleting all reservoir storage in a given year) for Alternatives C and D. Same climate scenarios as in previous figure.....27

Figure 23: Boxplots showing the average delivery shortage volume in a 50-year period for alternatives A and B. (a) Natural variability only, no climate change induced flow reductions. (b) 10 percent climate change induced flow reduction. (c) 20 percent climate change induced flow reduction.....28

Figure 24: Boxplots showing the average delivery shortage volume in a 50-year period for alternatives C and D. (a) Natural variability only, no climate change induced flow reductions. (b) 10 percent climate change induced flow reduction. (c) 20 percent climate change induced flow reduction.....28

Figure 25: Boxplots showing the number of years with a delivery shortage in a 50-year period for alternatives A and B. (a) Natural variability only, no climate change induced flow reductions. (b) 10 percent climate change induced flow reduction. (c) 20 percent climate change induced flow reduction.....29

Figure 26: Boxplots showing the number of years with a delivery shortage in a 50-year period for alternatives C and D. (a) Natural variability only, no climate change induced flow reductions. (b) 10 percent climate change induced flow reduction. (c) 20 percent climate change induced flow reduction.....29

Figure 27: Boxplots showing the showing the total volume of flow from the Gila River in a 50-year period under the three climate change scenarios (a) Natural climate Variability only; (b) 10 percent climate change induced reduction of flow; (c) 20 percent climate change induced reduction of flow.....30

Abstract

As the annual demand on the Colorado River system approaches the annual supply, the contribution from the Lower Colorado River Basin (LCRB)—on average about 15 percent of total system flows—becomes more critical. In order for these flows to be incorporated into planning frameworks, it is important to understand their long-term variability and develop robust simulation methods that can capture the variability. The main objectives of this project were to develop new paleo-reconstructions of LCRB hydrologic variability from tree rings and incorporate them into a more complete assessment of the risk for the entire Colorado River Basin.

We first worked to develop or refine naturalized flow records for the Gila and non-Gila subbasins of the LCRB. We found that while the historic Gila River naturalized flows near the mouth could be estimated with high confidence, the non-Gila LCRB flows carry more uncertainty. We then used several different statistical methods, including two new methods, to calibrate a regional network of tree-ring data against these naturalized flow records. The resulting flow reconstructions extend back about 400 years, and are more robust for the Gila River than the non-Gila portion of the LCRB. The reconstructions show that the 20th century has been unrepresentative of the longer period of hydrologic variability in several key respects. We then incorporated the variability in these new tree-ring reconstructions into a more complete water-balance model simulating the managed Colorado River system, which was run under multiple future scenarios representing different levels of climate change impact and increasing demands. We found that the periodic large inflows from the Gila River have a small but measurable effect in reducing overall system risk (of depleting) storage under all scenarios.

1. Background and Justification

The Colorado River Basin (CRB) is the most important source of water in the southwestern United States, and the state of Colorado draws a substantial portion of its water supply from the CRB (Figure 1). Since the Upper Colorado River Basin (UCRB) provides, on average, 85 percent of the total CRB's annual flow in most years, previous investigations of water supply reliability for the CRB have focused on the UCRB. Given the smaller contribution of Lower Colorado River Basin (LCRB) flows, they have been typically left out of the CRB water supply modeling, or represented with constant terms. Also, the Gila River (Figure 1), which contributes about half of the LCRB flows, is not explicitly incorporated in the legal and management structure governing the rest of the CRB.

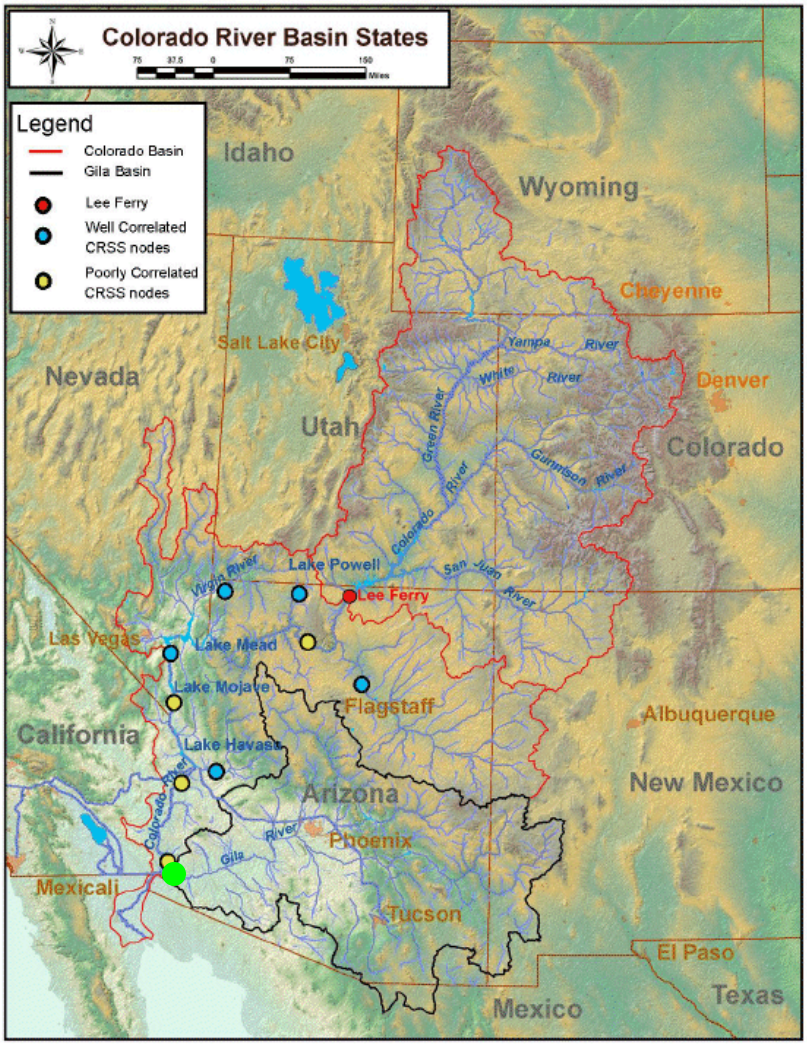

Figure 1. Colorado River Basin (CRB). The basin is divided at Lee(s) Ferry (red dot) for legal and management purposes into an UCRB and LCRB (red boundaries). The watershed of the Gila River is outlined in black, with the Gila near Dome, AZ gage shown in green. USBR's nine CRSS model nodes in the LCRB are shown as blue and yellow dots. The intervening flows at the five blue nodes are well correlated with precipitation while the four yellow nodes are not. We used only the five blue nodes to calibrate the Lower Colorado mainstem flow reconstruction. See further details in the text.

However, as the demand on the CRB system approaches the supply, the contribution from the LCRB—which averages 15 percent but has varied from six percent to over 30 percent depending on the year—becomes more critical. In order for these flows to be incorporated into planning frameworks, it is important to understand their long-term variability and develop robust simulation methods that can capture the variability. Observed flow data that are limited in time (~100 years) cannot provide the full range of variability, even with stochastic models built on them. Paleohydrologic reconstructions of annual flow using tree rings, however, provide much longer (500–1000+ years) records of past natural variability, and thus a much richer sampling of potential flow sequences, including severe and sustained droughts of greatest concern to water resource managers. Multi-century tree-ring reconstructions of the annual water year flow of the Colorado River at Lees Ferry which capture the contributions from the UCRB have been developed (Woodhouse et al. 2006; Meko et al. 2007) and have been used in previous efforts to assess CRB water supply reliability (Reclamation, 2007; Barnett and Pierce 2009; Rajagopalan et al., 2009). Thus, the overall objectives of this project were to develop new paleo-reconstructions of LCRB hydrologic variability, commensurate with the reconstructions at the Colorado River at Lees Ferry, and incorporate them into a more complete assessment of the risk for the entire basin. The project was motivated in large part by interests of the Colorado River District (CRD), which is responsible for the conservation, use, protection, and development of Colorado's apportionment of the Colorado River.

2. Methods and Results

To meet the objectives of the project, a sequence of work was performed that can be summarized as follows. The sequence and interaction of the steps is shown schematically in Figure 2.

- Compile the available tree-ring chronologies within and adjacent to the LCRB
- Conduct analyses of gaged flows in the LCRB, and develop naturalized annual flow records for the LCRB for the historic period (~1906 to present) to use as targets for the paleohydrologic (tree-ring) reconstructions, for these two locations:
    - The flow for the Gila River near its confluence with the Colorado
    - The intervening flow on the Colorado River between Lees Ferry and Imperial Dam
- Generate and evaluate paleohydrologic reconstructions for Gila flows and the mainstem intervening flows using multiple methods
- Perform system response analysis using the new LCRB reconstructions as input to Rajagopalan et al. (2009) water-balance model of the CRB

The methods and results for the main components of the project are described in the following subsections. Additional details can be found in Wade (2012).

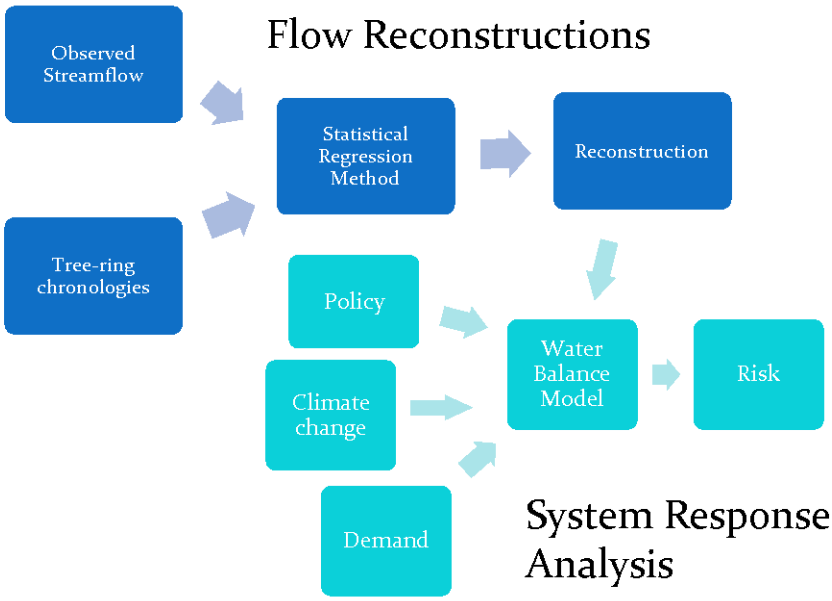

Figure 2. Schematic showing the development of the streamflow reconstructions (dark blue) and their subsequent use as one of the inputs into the system response analysis (light blue).

2.1 Tree-ring reconstructions – background on methods and previous work

Tree-ring reconstructions of streamflow are based on site *chronologies*, in which the ring-width measurements of 10–30 or more moisture-sensitive trees at a given site are corrected for non-climatic growth trends and then composited to produce a time-series of dimensionless ring-width indices that captures the common climate signal in the trees (Cook and Kairiukstis, 1990). Most typically, a regression equation is fitted, or calibrated, between an observed streamflow record and either a subset of available chronologies for the region, or principal components derived from those chronologies. Then the full lengths of the chronologies are applied to the equation, generating estimates of streamflow back in time. A more detailed explication of the general methodology can be found in Meko and Woodhouse (2011).

Generally, observed streamflow records used for calibration must be naturalized to remove the effects of depletions, diversions, reservoir operations, and the like. Since these human effects on hydrology are not recorded by the trees, their presence in the streamflow record would introduce error into the reconstruction.

There have been previous efforts that have successfully reconstructed streamflows for parts of the Gila River Basin using tree rings (Smith and Stockton 1981; Meko and Graybill 1995; Meko and Hirchboeck 2008). These efforts focused on headwaters gages and did not attempt to reconstruct the flows at the mouth of the Gila River under natural or managed conditions. Similarly, there have been several previous efforts to reconstruct flows in parts of the non-Gila portion of the LCRB, but not to reconstruct the total flows between Lees Ferry and Imperial Dam.

2.2 Development of naturalized observed flow records

2.2.1 Gila River

The hydrology of the Gila River is almost entirely modified by reservoir operations and depletions before it joins the Colorado River, and these modifications began in the first decade of the 1900s. Several headwater gages on the mainstem Gila and its major tributaries (Salt River, Verde River, Tonto Creek) are above the dams and most diversions and remain mainly natural (Figure 3).

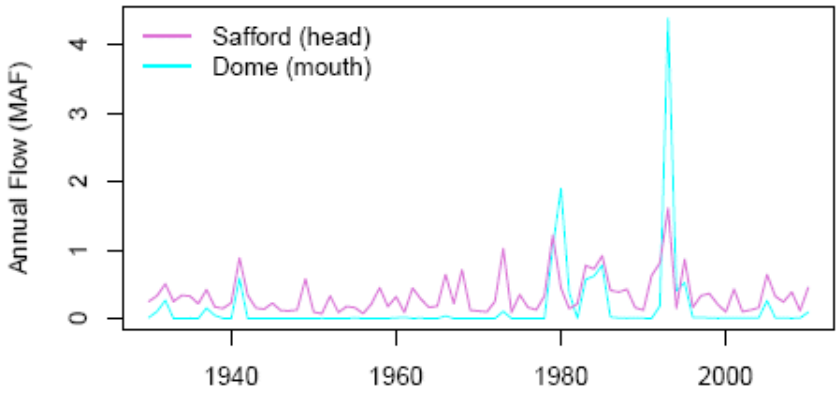

Figure 3. Gaged annual streamflows (1929–2011; USGS) for the Gila River at two gages: Safford Valley, near Solomon, AZ, in the headwaters of the basin (red); and near Dome, AZ, at the confluence of the Gila and the Colorado River (blue). The flows at Safford represent near-natural conditions; intensive use of the river downstream of Safford has resulted in flows at the mouth that are near-zero in most years, spiked with periodic very large flows, such as in 1980 and 1993.

The gage record closest to the mouth of the Gila is near Dome, AZ (Figure 1). The Bureau of Reclamation (Reclamation 1946) developed estimates of natural flow at gages downstream of the dams and diversions, including the gage near Dome, AZ (the closest gage to the mouth), for the period 1897–1943. After extensive analysis of the gaged records for the Gila River Basin, we developed a local polynomial regression model between the USBR-estimated naturalized flow near Dome for the 1897–1943 period and the near-natural gaged flows at the headwater gages. This regression performed very well, with an R^2 of 0.89, and the validation diagnostics were also good; see Wade (2012). The modeled estimated natural flows for the Gila near Dome cover the period 1915–2010 (Figure 4). The mean annual flow for the 1915–2010 period is 1.1 million acre-feet (MAF), but it varies from 0.04 MAF to over five MAF.

It should be noted that the naturalized flows near Dome are significantly lower than the natural flows higher in the basin, due to channel losses below the Phoenix area that were estimated by Reclamation (1946) at 1.0 MAF/yr. Assuming this loss term to be robust, the naturalized flow in the Phoenix area can be estimated at 2.1 MAF/yr over the 1915–2010 period; Reclamation (1946) estimated a Phoenix-area flow 2.3 MAF/yr over the shorter, and generally wetter, 1897–1943 period. These estimates of Phoenix-area flow are consistent with the aggregate observed

flow at the four headwaters gages of 1.5 MAF/yr over the 1915–2010 period; there are several important tributaries that enter the Gila River below those gages.

As a check on the reliability of these estimated natural flows, we obtained from the Bureau of Reclamation natural streamflows for the Dome gage as modeled by the Variable Infiltration Capacity (VIC) macroscale hydrology model, for the water years 1950–1999 (S. Gangopadhyay, personal communication). The VIC model uses observed monthly precipitation and temperatures as inputs. While the average magnitude from our estimates and from the VIC model did not agree well, the *variability* was extremely similar (R^2 = 0.95), giving us confidence that our estimated flows at mouth were consistent with observed hydroclimate over the basin.

We also retained the gaged flow record at Dome (1930–2011; Figure 3) as a second calibration series since the gaged flows represent the inputs to the Colorado from the Gila under current, managed conditions and thus are more relevant for the system risk model as we implemented it.

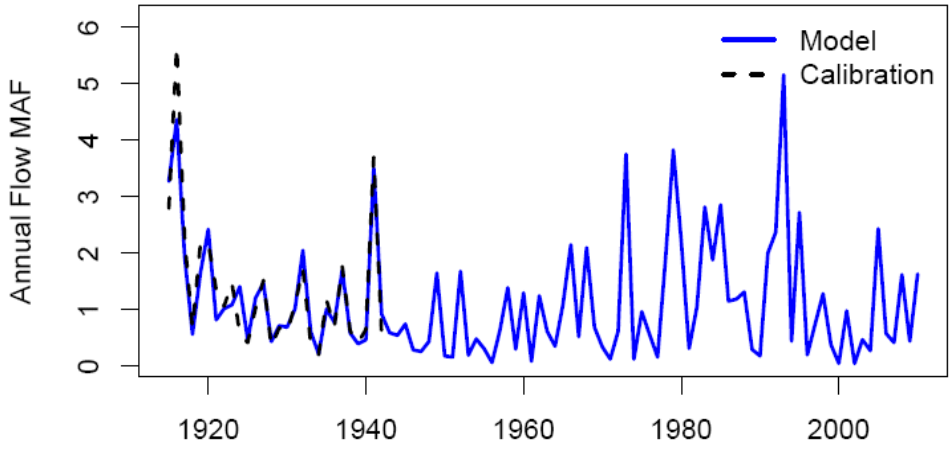

Figure 4. Our model (blue) of estimated natural annual streamflows (1915–2010) for the Gila River near Dome, AZ, at the confluence of the Gila and the Colorado River. The model predictors are gaged headwaters flows, including the Safford gage shown in Figure 2, calibrated on natural flows for 1897–1943 estimated in Reclamation (1946) (dashed black line).

2.2.2 Mainstem Lower Colorado River

The US Bureau of Reclamation maintains and periodically revises a "natural flow" dataset for the Colorado River and major tributaries for the 29 input nodes for their CRSS system model, for 1906–2008. While for the 20 nodes in the UCRB the flows have been explicitly naturalized, this is not the case for the nine nodes in the LCRB (see Figure 1). Four of these nodes correspond to USGS gages near the mouths of major tributaries, and for these four nodes, the gaged flows (statistically extended to the full 1906–2008 period as needed) are used as the natural flows. In fact, there are depletions in these tributaries that are not accounted for. The other five nodes represent intervening flows along the mainstem Colorado, in principle reflecting inputs from minor tributaries and also channel losses and other natural losses. Natural flows at these five

nodes are calculated using a water-balance model with architecture and function similar to the CRSS model. The necessity of reconciling the total flows entering the "top" of the LCRB at Lee Ferry with those gaged at the "bottom" at Imperial Dam means that the calculated intervening flows at each of these five nodes likely contain artifacts of the water-balance modeling. In effect, gaging error and other errors which may be acceptable in the context of the total flows (average: 15–17 MAF) are carried over in the derivation of the much smaller (<1 MAF) intervening flows at these five nodes, and become relatively larger.

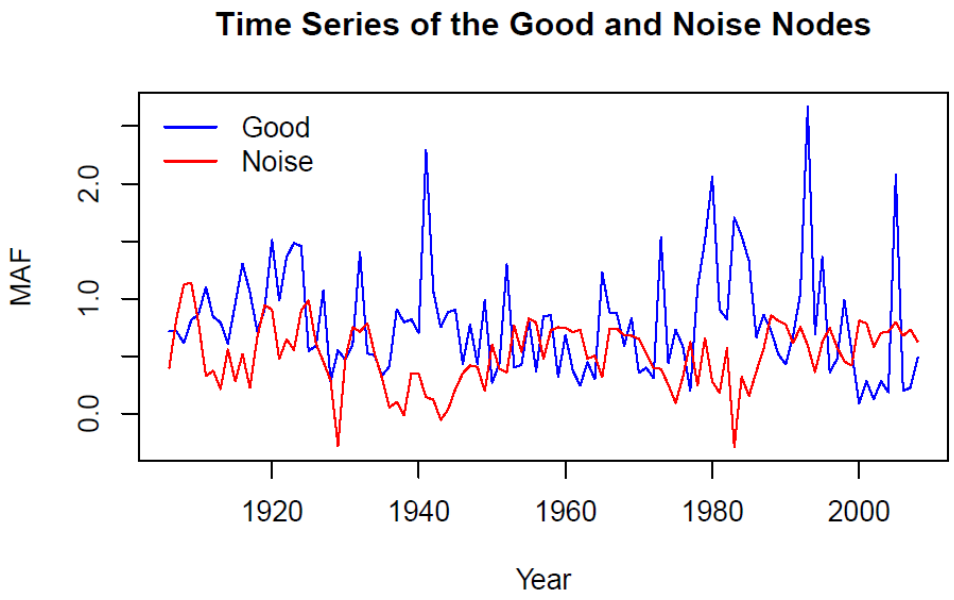

Figure 5. The natural flows for the nine nodes of the CRSS model in the Lower Colorado Basin fell into two groups: five good nodes whose flows are well-correlated with observed hydroclimate in the basin, and four noise nodes, whose flows are not.

We conducted correlation analyses of the "natural flows" at all nine nodes, and discovered that flows at five nodes from 1906–2008 were well correlated ($r > 0.5$) with both observed precipitation and streamflow in adjacent basins. These five "good" nodes include all four nodes representing the major tributaries, and one of the mainstem intervening flow nodes. But the flows at the other four nodes—all mainstem intervening flows—were essentially uncorrelated (r = ~0) with observed hydroclimate, and very poorly correlated with the total of the good nodes (Figure 5) and we refer to these as the "noise" nodes. The good nodes represent about 60 percent (0.81 MAF) of the total flow at all nine nodes (1.31 MAF), and the noise nodes about 40 percent (0.50 MAF). We also found that the total flows at the good nodes were very highly correlated with flows simulated by the VIC hydrology model ($R^2 = 0.75$), and as expected, this fit was degraded when the flows at the noise nodes were added. Thus, we retained only the flows at the five good nodes to represent the Lees Ferry to Imperial reach, for calibration with the tree-ring data.

Since the five-node total flow is less than the value used to represent the total mainstem flows in previous risk assessment studies, to make our results comparable with the previous work we added a white noise term averaging 0.50 MAF to the tree-ring reconstruction of the five-node

flows, as described in section 2.7.2. This is not the most satisfactory solution, since the robustness of the 1.31 MAF figure is uncertain. The Reclamation (1946) report cited above also estimated the natural flows of the mainstem below Lees Ferry. The natural flows from Lees Ferry to Lake Mead for 1897–1943 were estimated at 1.06 MAF/yr, slightly higher than the sum of the flows at the five nodes above Lake Mead (0.86 MAF/yr) over the 1906–2010 period. Given that the latter period was slightly drier overall, there is reasonable agreement on the flows above Lake Mead. For the reach below Lake Mead to Laguna Dam, Reclamation (1946) estimated that the gross inflows were 0.15 MAF/yr, compared to the 0.45 MAF/yr value for the four nodes below Lake Mead in the current Reclamation natural flows database. Given that three of these four nodes were found to be "noise nodes" in our analysis, the 0.45 MAF/yr value is suspect.

2.3 Compilation of tree-ring chronologies

Long-lived, moisture-sensitive conifers are widespread in the LCRB and adjacent areas of Arizona, New Mexico, Utah, and Colorado. We recompiled a total of 61 tree-ring chronologies that had been recently collected and developed for three other projects: The Salt River Project (SRP)-LTRR Project (Meko and Hirschboeck 2008), the North American Monsoon project (Griffin et al. 2011), and the Non-Parametric Project (Gangopadhyay et al. 2009). Most of the chronologies extend back before 1600, and about one-third extend before 1500, with five chronologies extending back before 1000. Nearly all of the chronologies end in 2002 or later, with most ending between 2005 and 2010. All of the chronologies are significantly correlated with observed water-year precipitation over the LCRB (1896–); average correlation $r = 0.53$.

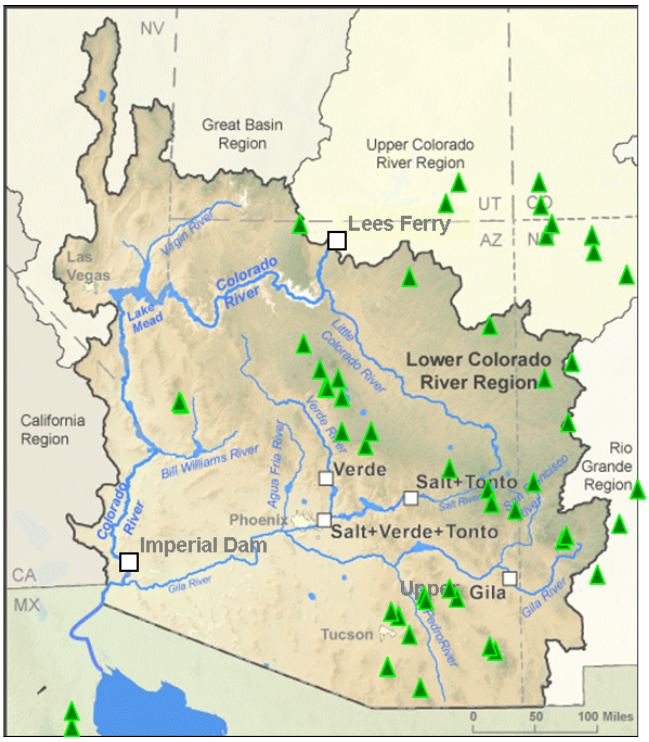

Figure 6. The locations of the 61 tree-ring site chronologies whose data were compiled for this study (green triangles).

Most of the chronologies are located within the LCRB, and are concentrated in the Four Corners region of the Colorado Plateau, the Mogollon Plateau in central Arizona, and the Sky Islands of southeastern Arizona (Figure 6). Relatively few, however, are in the non-Gila portion of the LCRB. Nearly all of the chronologies are ponderosa pine (*Pinus ponderosa*), pinyon pine (*P. edulis*) or Douglas-fir (*Pseudotsuga menziesii*). Jeffrey pine (*P. jeffreyi*), sugar pine (*P. lambertiana*) and white fir (*Abies concolor*) are represented by one chronology each.

2.4 Generation of Tree-ring Reconstructions

2.4.1 Overview of methods

Paleohydrologic reconstructions from tree rings have been generated using many different statistical approaches, all of which have particular strengths and weaknesses. The most straightforward and commonly used approach has been multiple linear regression (MLR; e.g., Woodhouse and Lukas 2006; Meko and Graybill 1995; Gray et al. 2011). The observed streamflow record used as a calibration target must first be checked for normality. If the flows are not normally distributed, then a transformation to achieve normality, such as a log transform, is applied. The linear regression model is fitted to the transformed flows and then back-transformed (Woodhouse and Lukas 2006). Based on the autocorrelation structure of the streamflow, prewhitened ("residual") or non-prewhitened ("standard") versions of the chronologies can be used in the regression. If there is no significant autocorrelation, residual chronologies are used (Cook and Kairiukstis 1990). Lagged predictors may be included in the pool of potential predictors in order to incorporate any carryover effects (Meko and Graybill 1995). The set of best tree-ring chronologies to enter the model are typically determined in a stepwise manner by a partial F-test, ensuring that the model is not overfitted. Models are validated using a variety of methods, but generally either split-sample validation (Meko and Graybill 1995) or leave-one-out cross-validation (Woodhouse and Lukas 2006) is performed.

One of the potential problems with the multiple linear regression techniques is multicollinearity. Multicollinearity occurs when several highly correlated predictors are included in the regression model and can lead to overfitting (Hidalgo et al. 2000). To correct for this, a Principal Component Analysis (PCA) regression (PCAreg) has also been employed (Fritts 1976). The use of PCA reduces the set of chronologies to a much smaller number of principal components (PCs) that capture the primary modes of variability. The PCs are then used as predictors in a multivariate regression model, eliminating multicollinearity and creating a more parsimonious model (e.g., Stockton and Jacoby 1976; Hidalgo et al. 2000; Woodhouse et al. 2006).

PCAreg, however, does not resolve other general limitations of linear regression techniques, including the assumption of normal distribution, the inability to capture nonlinear features in the observed data, and outliers having undue influence on the global model fit. Recently, two additional methods that address these limitations have been employed for streamflow reconstruction. Gangopadhyay et al. (2009) developed a nonparametric approach in which a *K*-nearest neighbor (*K*-NN) resampling method is employed within the PC-space to resample historic natural flows to produce streamflow ensembles for each year. The advantages of the nonparametric approach are: no prior assumption of distribution of the variables, nonlinearities can be easily captured, and the influence of outliers is dampened. Prior to its use in streamflow reconstruction, the *K*-NN approach had been extensively used in stochastic streamflow

simulation (Lall and Sharma 1996; Rajagopalan and Lall 1999). The main drawback of the K-NN approach, being based on conditional resampling of the observed flows, is that only flow magnitudes within the range of the observed flow record can be generated. Back in the parametric realm, Meko and Hirschboeck (2008) employed a variant of multiple regression in which a LOWESS (locally weighted scatterplot smoothing) curve, rather than a straight line, is used to fit the regression model. This allows non-linear features in the relationship between the tree-ring data and the observed hydrology to be represented in the model.

For this project, we further expanded the repertoire of tree-ring paleohydrology with two new methods. The first method, referred to as 'Local Poly', is effectively a modification of the *K*-NN resampling scheme. In principle, it combines the best features of non-parametric approaches with those of the most flexible parametric approaches, such as the LOWESS regression. A local polynomial is fitted to the *K*-nearest neighbors, providing the ability to extend reconstructed values beyond the range of the observed data, while also capturing nonlinearities in the tree-ring/streamflow relationship. This method has been successfully used for stochastic streamflow simulation (Prairie et al. 2006) and streamflow forecasting (Grantz and Rajagopalan 2005; Regonda et al. 2006; Bracken et al. 2010). The second method uses extreme value analysis (EVA) to reconstruct threshold exceedances of streamflow. The motivation for this method is that annual streamflow records with high intermittency (e.g., near-zero annual flows in most years, with occasional high-flow years, as in the Gila gaged flow record) are difficult to fit using traditional methods. The EVA models the probability of threshold exceedance and the magnitude of exceedances. It is especially well suited for reconstructing intermittent processes, and applications in basins where management outcomes are sensitive to threshold exceedance, such as the Gila River.

To establish a baseline for comparison with the newer approaches, our collaborator Connie Woodhouse used two variants of the forward-stepwise MLR (standard and PCAreg) to reconstruct the naturalized streamflows for both sub-basins. Table 1 shows the additional approaches that were used for one or more of the three calibration hydrologies.

Table 1. Matrix showing the observed streamflow time-series (columns) that were reconstructed using one or more of the statistical approaches (rows). (Reconstruction generated by C. Woodhouse, University of Arizona; ** reconstruction generated by D. Meko, University of Arizona; all others generated by L. Wade)*

Approach	**Gila naturalized**	**Gila gaged**	**LCRB naturalized**
Forward-stepwise MLR	√*		√*
Forward-stepwise PCAReg MLR	√*		√*
LOWESS multiple regression	√**		
K-NN non-parametric	√		√
Local Poly	√		√
Extreme Value Analysis (EVA)	√	√	

Additional details on the newer approaches as they were employed for the study are provided below.

2.4.2 LOWESS multiple regression

Our collaborator David Meko developed this reconstruction using a multi-step procedure. First, 61 separate regression reconstructions were performed between the individual chronologies and the log-transformed flows, and then back-transformed. Then multiple LOWESS-smoothed multiple linear regression models were performed between time-varying subsets of these 61 single-chronology reconstructions and the untransformed flows. The final reconstruction is a time-nested combination of 22 different LOWESS MLR models, together covering all of the years 760–2010. While this reconstruction is very long, prior to 1500 the robustness of the sub-models declines significantly. The most robust sub-model is the one which covers the years 1600–1990, a period comparable to the other reconstructions.

2.4.3 K-*NN non-parametric*

This approach was performed using the same steps as described in detail in Gangopadhyay et al. (2009). In brief, "neighbors" (i.e., years in the calibration period) for each year in the reconstruction period were identified in a mutually orthogonal eigenspace and were conditionally bootstrapped to provide ensembles. The selection of neighbors was guided only by the tree-ring data, not by the observed flows. Essentially, the pattern of association between the chronologies in the calibration period and the reconstruction period was identified for each year in the reconstruction. This information is the foundation of the reconstruction process from which analog streamflow values are selected for each of the reconstruction years.

2.4.4 Local Poly - PCAreg

For this approach and the Extreme Value Analysis approach, we first screened the set of 61 chronologies for location and length, and retained 35 chronologies for further analysis. All of the 35 chronologies extend from at least 1612 to 2005. PCA is typically performed on an entire regional tree-ring dataset to reduce the number of independent variables to be used in the reconstruction model. To better capture local expressions of the climate signal embedded in the regional data, we first employed a cluster analysis on the tree-ring chronologies, using *k*-means clustering (Everitt et al. 2001). This method seeks clusters such that the sum of squared distances between the cluster centroid and cluster members (within sum of squares or *wss*) is minimized, while the distances between cluster centroids are maximized.

These two objectives lead to homogeneous and coherent groups that capture the spatial heterogeneity. PCA was then performed on each tree-ring chronology cluster separately, which enabled us to extract more of the climate signal from the entire tree-ring domain. The eigenvalues are ordered and provide the fraction of variance captured by the corresponding PCs. The leading PCs typically capture the majority of the variance and can be used in the subsequent regression model.

The major drawback to parametric regression is its inability to deal effectively with nonlinear relationships between independent and dependent variables, and the assumption of normality,

which is often violated by the dependent variables, such as streamflow—as is the case for the Gila River. Therefore, we used a local polynomial regression method within a Generalized Linear Modeling (GLM) (McCullagh and Nelder 1989) framework. In a GLM, the response or the dependent variable Y can be assumed to be a realization from any distribution in the exponential family with a set of parameters (McCullagh and Nelder 1989). A link function transforms the conditional expectation of Y to a set of predictors. The GLM can be used to model a variety of response variables; for skewed variables with a lower bound of zero such as streamflow, the Gamma distribution and its associated link function are appropriate and so it was used.

To retain local nonlinear features, a local fitting method was used instead of a global fit. This local polynomial provides an additional degree of flexibility to the GLM framework. The 'best model' consists of the local polynomial parameters (á and p) and the set of predictors that minimizes the Generalized Cross-Validation (GCV) criteria (Regonda and Rajagopalan 2004). Local polynomial based function estimation has been successfully used for streamflow forecasting, simulation, flood frequency estimation, water quality threshold exceedance, and stream temperature attributes (Regonda et al. 2006; Grantz et al. 2005; Bracken et al. 2010; Apipattanavis et al. 2010; Towler et al. 2010a, 2010b; Caldwell et al. 2012). This was its first use in paleohydrologic streamflow reconstruction.

The local polynomial approach is an improvement over the *K*-NN based resampling method of Gangopadhyay et al. (2009) because values can be obtained beyond the range of the observed data and noise can be smoothed out. Additional details of the method can be found in Wade (2012).

2.4.5 Extreme Value Analysis (EVA)

One model of the family of Extreme Value Analysis (Coles 2001) models, called Peaks-Over-Threshold (POT), was used. In this model, a threshold is selected and two components are modeled: (1) the probability of exceedance or non-exceedance of the threshold and (2) the magnitude of threshold exceedances when there is an exceedance, described by a Generalized Pareto Distribution (GPD) (Coles 2001)). The threshold can be user-specified, e.g., a threshold with particular significance in a decision-making context, or it can be selected in a quasi-objective manner. In the latter, different thresholds are selected and for each, the scale parameter is estimated. The region where the parameter remains stable is used to select the threshold. Selecting a threshold that combines these two objectives is usually preferred.

A companion procedure for the occurrence of exceedance is necessary to complete the model, which is typically modeled as a Poisson Process (Katz et al. 2002; Coles 2001) or as a logistic regression. Here, we modeled the probability of exceeding the threshold with a logistic regression. The observed natural flow time series is converted to a binomial variable with 1 representing an annual water year flow that exceeded the threshold and 0 representing a year that did not exceed the threshold. The logistic regression model was a GLM framework using a Binomial parent distribution with a logit link function. Additional details of the method can be found in Wade (2012).

2.5 Intermediate Modeling Steps

2.5.1 Local Poly - PCAreg

Cluster analysis was performed on the set of 35 tree-ring chronologies to separate the chronologies into three clusters, as shown in Figure 7. The clusters are focused on the plateau region of the Four Corners, the summer monsoon region in Arizona, and western New Mexico, respectively. PCA was performed on the chronologies in these clusters separately, and the leading three PCs for each cluster, which together explained 73 percent to 86 percent of the variance, respectively, in each cluster, were retained for further modeling.

Figure 7. The results of the k*-means cluster analysis on the 35 screened chronologies. Three clusters (colored ovals) were discerned, with two of them producing spatially contiguous groupings.*

The three leading PCs from each cluster were used as predictors in the local polynomial regression with normal parent distribution and identity link function. Based on the GCV criteria the best model had Alpha of 1, polynomial of degree 1, predictor set consisting of PCs 1, 2, and 3 from tree-ring cluster 2 and PC 1 from tree-ring cluster 3, and used a identity link function on the log transform of the flows assuming a normal distribution.

2.5.2 Extreme Value Analysis

For the gaged flows of the Gila River, a threshold of 0.2 MAF was selected since guidance from Reclamation engineers indicated that this was the minimum inflow from the Gila that could influence the operation of Hoover Dam. The shape and scale parameters of the GPD were stable in this range as well. For the nonstationary GPD model, the flow at the Roosevelt gage on the

Salt River was selected as the best covariate from the likelihood ration test, to model the scale parameter. The reconstruction of the Salt River from Meko and Hirschboeck (2008) was used to provide an estimate for the scale parameter of the GPD going to back to 1612. For the logistic regression model for the probability, the local polynomial model with a logit link function obtained the best parameter of α of 0.7, a polynomial degree of order 1, PC 1 from cluster 1, PC 2 and 3 from cluster 2, and PC 1 from cluster 3 were selected as best predictors.

For the naturalized flows of Gila River, the GPD parameters are fairly stable in the 1.5–2.5 MAF range, so we selected the mid-range figure of two MAF as the threshold. For the nonstationary GPD model, PC 1 from cluster 2 was selected as the best covariate from the likelihood ratio test, to model the scale parameter (see equation 3). Thus, for each year, the value of covariate from the tree ring chronologies provides an estimate of the scale parameter of the GPD, thereby, providing an appropriate GPD to describe the threshold exceedance flows for each year. For the logistic regression model for the probability of threshold exceedance, the local polynomial model with a logit link function obtained the best parameters α of 0.7, a polynomial degree of order 1, and PC 1 from clusters 1, 2, 3, PC 2 from cluster 3 as best predictors.

2.6 Results – Tree-Ring Reconstructions

2.6.1 Gila River – Naturalized Flows

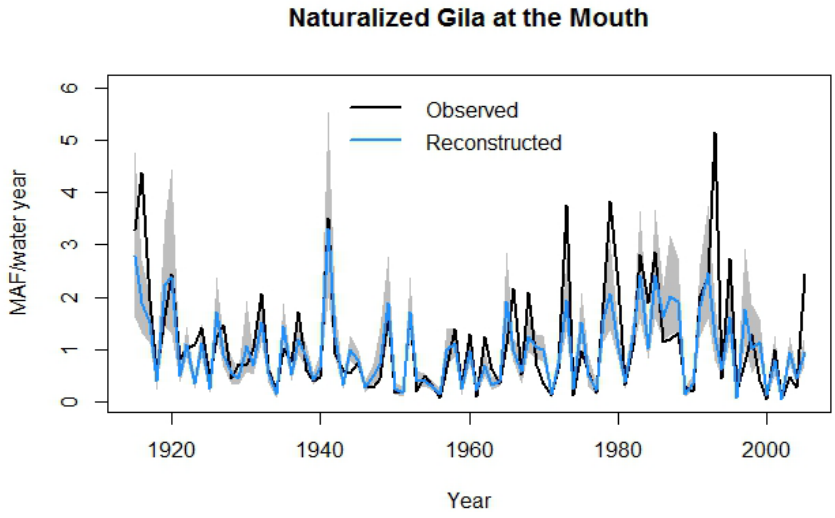

Figure 8. The Local Poly reconstruction model (blue) compared with the observed (naturalized) Gila River flows (black) over the calibration period of 1915–2005. The gray band is the confidence interval around the reconstructed values. This model captures the low flows extremely well, but tends to underestimate the high flows, particularly in 1993.

Because it is one of the two new methods, we first show the Local Poly tree-ring reconstruction (1912–2005) for Gila River near Dome naturalized flows, in Figure 8. This reconstruction tracks the observed variability very well, with an explained variance (R^2) of 0.55. The reconstruction captures the low flows extremely well, but tends to underestimate the high flows, particularly in 1993. The Local Poly method has the added benefit of providing a variable confidence interval

width (grey shading). The level of confidence in the predicted values changes over time depending on the spread among the tree-ring data contributing to a given year's value.

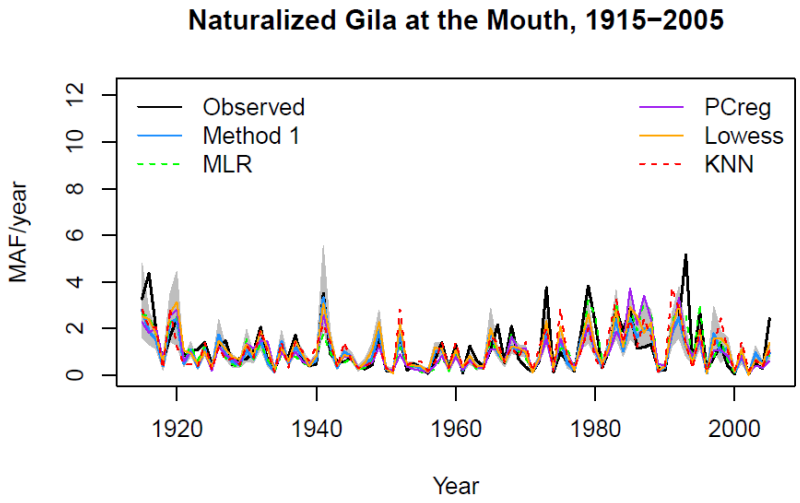

Figure 9. Five different reconstruction models, compared with the observed (naturalized) Gila River flows over the calibration period of 1915-2005. (Method 1 is the Local Poly method.) All of the models capture the low flows better than the high flows, which are consistently underestimated.

The broader ensemble of tree-ring reconstructions of Gila River near Dome naturalized flows over the calibration period of 1915-2005 are shown in Figure 9. Five of the six reconstruction methods which were applied to this flow record are shown, excluding only the EVA-POT method, which is shown separately later. They explain between 41 percent and 61 percent of the variance in the observed flows, respectively. Over the calibration period, all five reconstructions track each other well, reflecting the robustness of climate signal contained in the tree-ring network to the different methodologies. All five reconstructions closely capture the magnitude of the low flows, but there are greater deviations in the high-flow years. Notably, all five methods fail to capture the magnitude of the extreme high-flow year in 1993.

The full reconstruction (1612–2005) of naturalized annual Gila River flows using the Local Poly method is shown in Figure 10, and the ensemble of all five reconstructions is shown in Figures 11 (annual values) and 12 (5-year running means). As with the calibration period, all five reconstructions track each other fairly well, testifying to the robustness of the underlying tree-ring signal. Some features common to the reconstructions are worth noting: (1) several of the reconstructed high flows before 1900 are higher than 1993; (2) there are several periods of persistent low flows before 1900 more protracted than those after 1900; and (3) the two multi-decadal periods of relatively high flows in the 1900s (*c.* 1900–1920 and 1970–2000) make the 20th century appear to be anomalous compared to the previous three centuries. The mean and median reconstructed flow is also generally lower before 1900 than after 1900.

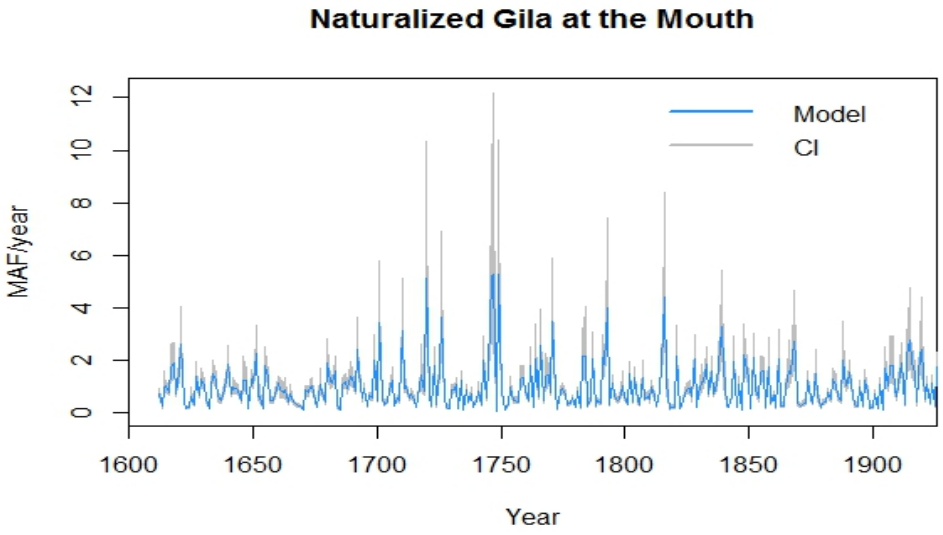

Figure 10. The Local Poly reconstruction of Gila River flows (blue), compared with the observed (naturalized) Gila River flows (black) over the period of 1612–2005. Note that the model generates high flows even higher than the 1993 observed flow.

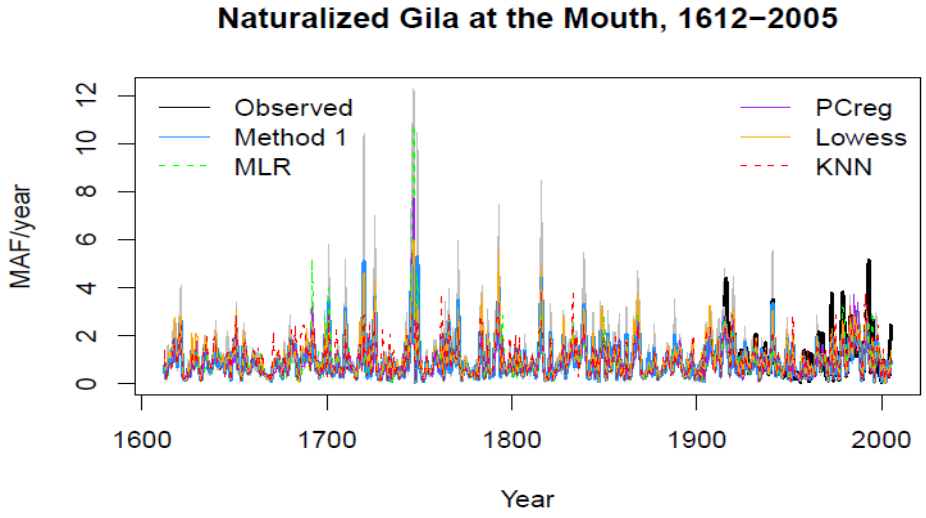

Figure 11. Five different reconstructions of annual Gila River flow, over the period of 1612–2005. (Method 1 is the Local Poly method.) The reconstructed variability is very similar among the reconstructions, with the reconstructed magnitudes differing most in the high-flow years.

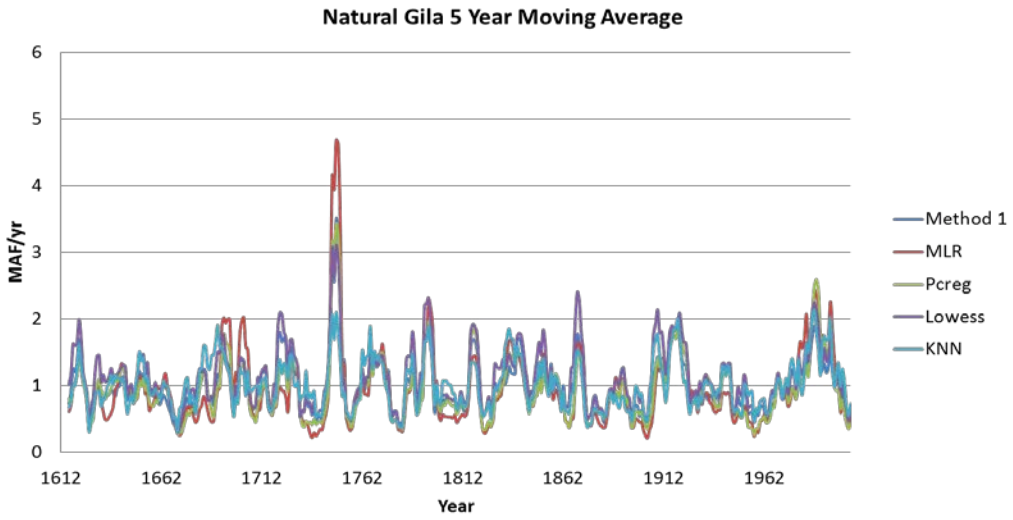

Figure 12. Five different reconstructions of annual Gila River flow, smoothed with five-year running averages, over the period of 1612–2005. (Method 1 is the Local Poly method.) The timing and magnitude of decadal-scale high- and low-flow periods is very similar, with the notable exception of the magnitude of the very high-flow period around 1750.

Since the methods of reconstructing the Gila River naturalized flows provide such similar results, and it is difficult to determine which is the "best" answer, we combined using a simple average the three reconstructions that explained the most variance: the MLR, the Lowess regression, and the Local Poly method. The combined reconstruction explains 62 percent of the variance in the observed flow record, slightly higher than any of the individual methods. Figure 13 shows the annual values and five-year running means for this combined reconstruction.

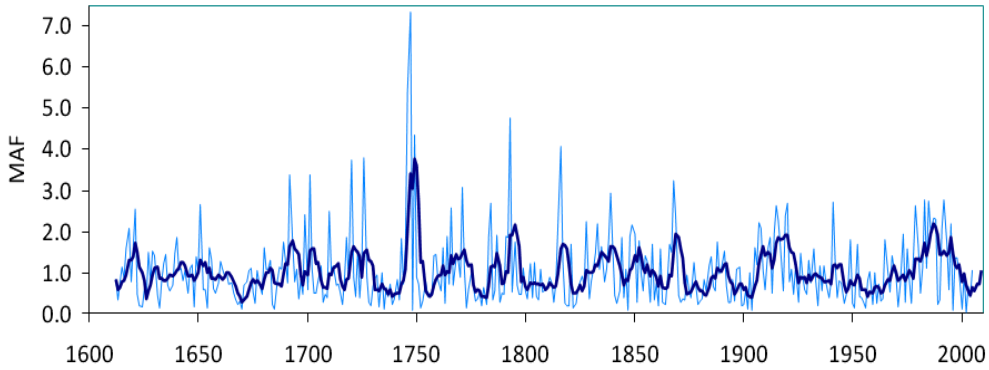

Figure 13. Combined three-method reconstruction of annual Gila River flow (see text) over the period of 1612–2005. The annual values are shown with the thin line, and the five-year running means with the thick line.

The Gila River reconstructions also demonstrate that the degree of similarity (and conversely, the differences) between the UCRB and LCRB hydroclimate as captured in the observed records extends into the paleo period. From 1915–2010, the observed Gila River naturalized flows and the observed Lees Ferry naturalized flows correlate at 0.54; over the longer 1612–2005 paleo

period, the reconstructed Gila River flows and the reconstructed Lees Ferry flows (Meko et al. 2007) correlate at ~0.5, depending on the specific Gila reconstruction.

The EVA-POT model of the naturalized Gila River flows is shown separately since it captures different aspects of hydrologic variability than the other reconstruction methods: (1) probability of exceeding the predetermined threshold (in this case, two MAF); and (2) the reconstructed flow magnitude in only those years which have a probability of exceedance greater than 0.2. Figure 14 shows the estimated probability of exceedance, and flow magnitudes, over the calibration period of 1915–2005. Of the 16 observed annual flows over two MAF, the model identified the probability of exceedance as being over 0.2 in 15 of those years (94 percent) and best-estimated annual flows over two MAF in those cases. It did, however, also estimate flows over two MAF for several years in which the observed flow was below two MAF.

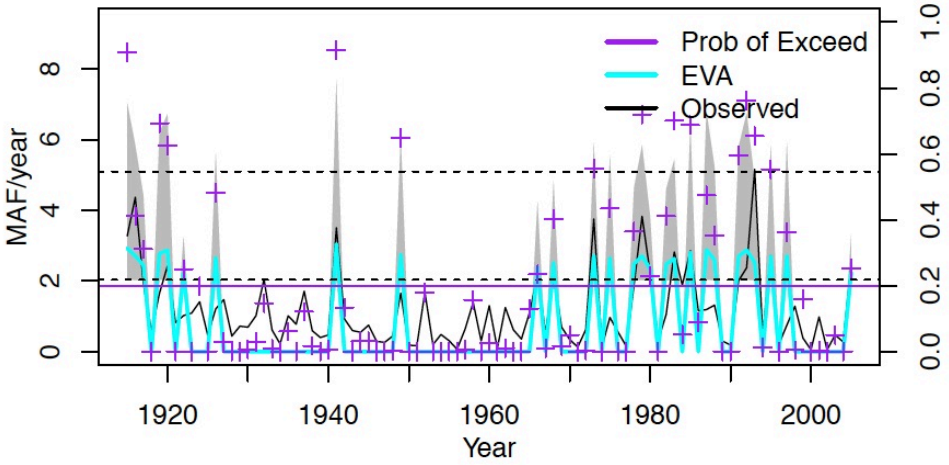

Figure 14. The Extreme Value Analysis Peaks-over-Threshold model compared to the observed (naturalized) Gila River flows over the calibration period of 1915–2005. The blue line is the reconstructed flow magnitudes (left-hand y-axis) and the purple crosses are the reconstructed probability of exceeding the threshold of two MAF.

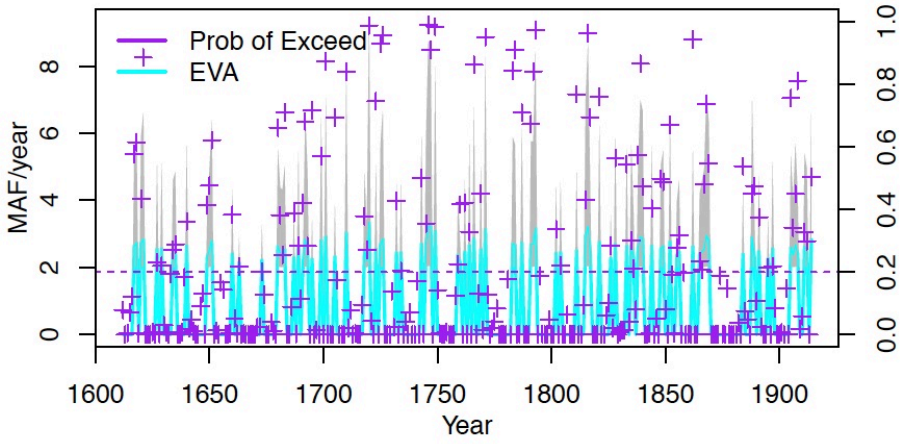

Figure 15. The Extreme Value Analysis Peaks-over-Threshold reconstruction of naturalized Gila River flows over the reconstructed period of 1612–2005. The blue line is the reconstructed flow magnitudes (left-hand y-axis) and the purple crosses are the reconstructed probability of exceeding the threshold of two MAF.

The EVA-POT reconstruction of the naturalized Gila River flows for the entire period of 1612–2005 is shown in Figure 15. It indicates that the flows over two MAF tend to be clustered in time, with periodic gaps between those clusters, most notably in the late 1800s.

2.6.2 Gila River – Gaged Flows

The EVA-POT method was the only method applied to the gaged Gila River flows because of the extreme intermittency of those flows. Figure 16 shows the estimated probability of exceedance, and flow magnitudes, over the calibration period of 1930–2005. Of the 12 gaged annual flows over 0.2 MAF, the model estimated the probability of exceedance as being 1.0 in all 12 of those years, and best-estimated flows over 0.2 MAF. It did not incorrectly estimate a probability of exceedance in any other years. As with the other reconstruction methods, the EVA-POT greatly underestimated the flow magnitudes in some of the very high-flow years, including 1980 and 1993.

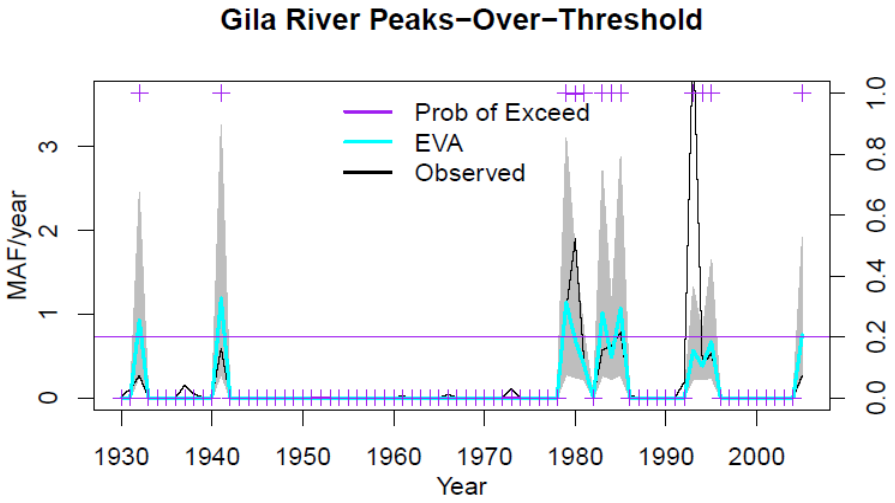

Figure 16. The Extreme Value Analysis Peaks-over-Threshold model compared to the observed (gaged) Gila River flows over the calibration period of 1930–2005. The blue line is the reconstructed flow magnitudes (left-hand y-axis) and the purple crosses are the reconstructed probability of exceeding the selected threshold of 0.2 MAF.

The EVA-POT reconstruction of the gaged Gila River flows for the entire period of 1612–2005 is shown in Figure 17. It indicates that if the modern management of the Gila River had occurred under the hydroclimate of the pre-1900 period, there would have been periodic inflows over 0.2 MAF from the Gila into the Colorado River, with about half of these inflows also exceeding 1.0 MAF, just as in the modern period. The frequency of reconstructed threshold-exceeding inflows is actually slightly higher during the pre-1930 period (one every ~5 years), compared to the post-1930 calibration period (one every ~6 years).

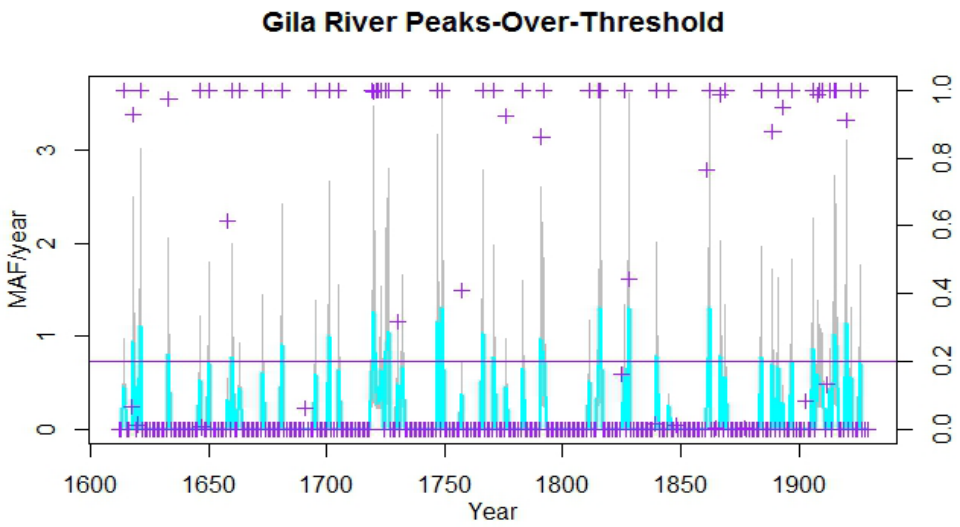

Figure 17. The Extreme Value Analysis Peaks-over-Threshold reconstruction of gaged Gila River flows over the reconstructed period of 1612–2005. The blue line is the reconstructed flow magnitudes (left-hand y-axis) and the purple crosses are the reconstructed probability of exceeding the threshold of 0.2 MAF.

2.6.3 Mainstem Lower Colorado River Flows – Naturalized Flows

The reconstructions of mainstem Colorado River flows (the five good nodes) are not quite as robust as the Gila River reconstructions, likely reflecting the inadequacies in the calibration flow record, as described earlier, and/or the drier and less snowmelt-driven hydrology of the non-Gila portions of the LCRB, which the trees would tend to not capture as well as the more snowmelt-driven Gila basin hydrology. The three-member ensemble of tree-ring reconstructions of the five-good-node flows over the calibration period of 1906-2005 is shown in Figure 18. They explain between 37 percent and 52 percent of the variance in the observed flows. As with the Gila, the low flows are reconstructed more accurately than the high flows.

The full reconstructions (1612–2005) of the five-good-node flows are shown in Figure 19. The reconstructed variability is less similar among the reconstructions than with the Gila reconstructions, reflecting that the tree-ring network is capturing the hydrology less robustly. As with the Gila reconstructions, the mean and median flows prior to 1900 are slightly lower than those after 1900. The similarity between the reconstructed mainstem LCRB flows and reconstructed Lees Ferry flows, as for the Gila, is comparable to than the similarity between the observed flows. From 1915–2010, the observed five-good-node flows and the observed Lees Ferry naturalized flows correlate at 0.54; over the longer 1612–2005 paleo period, the reconstructed five-good-node flows and the reconstructed Lees Ferry flows (Meko et al. 2007) correlate at ~0.6, depending on the specific five-good-node reconstruction.

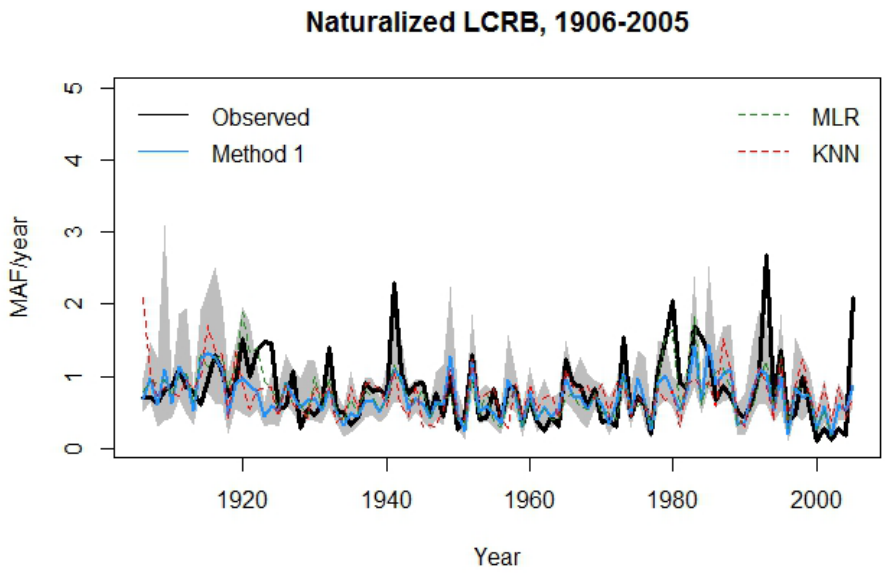

Figure 18. Three different reconstruction models, compared with the observed five-good-node LCRB (non-Gila) flows over the calibration period of 1906–2005. (Method 1 is the Local Poly method.) As with the Gila River, all of the models capture the low flows better than the high flows, which are consistently underestimated.

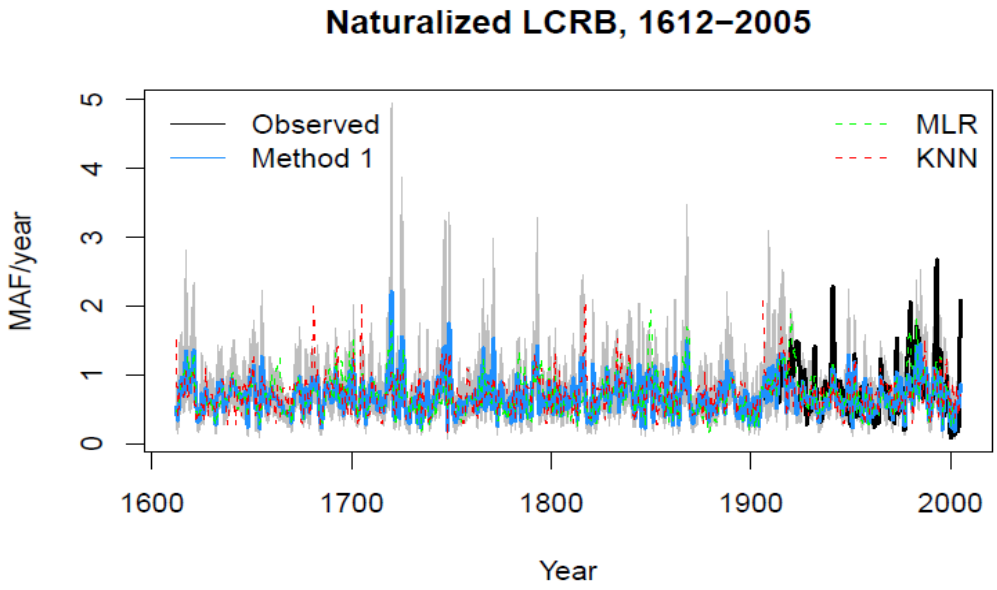

Figure 19. Three different reconstructions of annual five-good-node LCRB (non-Gila) flow, over the period of 1612–2005. (Method 1 is the Local Poly method.) The reconstructed variability is less similar among the reconstructions than with the Gila reconstructions.

2.6.4 Summary

The new reconstructions for the naturalized Gila River flows show, first, that the information about past hydroclimate variability contained in the regional tree-ring network is fairly robust to

the specific statistical method used to calibrate and reconstruct the flows. They also show that the 20th century is not a representative sample of the broader range of variability seen in the pre-1900 reconstructed flows, in several important ways. The EVA-POT reconstruction of Gila River gaged flows demonstrates, for the first time, the potential to use tree-ring data to reconstruct highly intermittent annual flow series. The reconstructions of the mainstem Lower Colorado (non-Gila) flows were likely constrained in quality by issues with the calibration flows. These new reconstructions for the LCRB also demonstrate that long-term hydrologic variability in the LCRB, while highly correlated with that in the UCRB, is different enough to justify including the former in system risk assessment as a complement to the latter. Further analyses of the reconstructions can be found in Wade (2012).

2.7 System response analysis

2.7.1 Background

In recent years, concern has been expressed regarding the ability of the CRB system to meet demands in light of high population growth in the basin as well as potential future changes in the flow regime caused by climate change. Several studies have used output from global climate models to investigate the impacts of projected warmer temperatures, combined with changes in precipitation, on CRB streamflows. These studies have generally projected reductions in annual flows of five to 25 percent by 2050 (Milly et al. 2005; Christensen and Lettenmaier 2007; Reclamation 2011a and 2011b).

The sustained drought in the 2000s served to highlight the potential vulnerability of the system. Recognizing the need to take additional management action, Reclamation, the seven Basin states (Arizona, California, Colorado, Nevada, New Mexico, Utah, and Wyoming), and other stakeholders agreed on the Interim Guidelines (Reclamation, 2007). This agreement outlines how to coordinate Lake Mead and Lake Powell operations until 2026, and mandates shared shortages in water deliveries to the LCRB when the level of Mead drops to certain thresholds (Reclamation, 2007).

Barnett and Pierce (2008) developed a simple model for the CRB water supply and tested it with stochastic streamflow simulations based on both paleo and observed data. Climate change impacts were modeled with a 10 percent and 20 percent linear reduction trend, with the full reduction occurring in the last year of a 50-year simulation. The 10 percent and 20 percent climate change reduction scenarios were based on the range of results from the explicit modeling studies mentioned above. Future demands were based on the projections from Interior (2007). The operating rules prior to the Interim Guidelines (which were not implemented at the time of their analyses) were modeled for reservoir operations. Their model consisted of Lake Mead storage with input from Lees Ferry. Barnett and Pierce (2008) found that there was a 50 percent probability of Lake Mead going dry by 2016 under a 20 percent flow reduction, a result which garnered substantial attention and criticism.

Barsugli et al. (2009) argued that the Barnett and Pierce (2008) system model had substantial shortcomings: it did not include other storage in the system, reservoir evaporation was improperly incorporated, and streamflows entering below Lees Ferry were modeled as a constant number and were too low. Consequently, the dramatic risk of drying under supply

reduction and demand growth was to be expected. Barsugli et al. (2009), using a system model addressing these issues, found that 50 percent probability of Lake Mead going dry occurs in the early 2030s under the same supply and demand assumptions.

Rajagopalan et al. (2009) expanded on this system modeling effort by including all of the storage in the system (60 MAF) and all the inflows (Lees Ferry streamflow and the intervening flows between Lees Ferry and Imperial Dam, the most downstream point on the system). Furthermore, they had a proper representation of reservoir evaporation and tested the system with five different reservoir operation and demand management scenarios, including the 2007 Interim Guidelines. They found that projected demand growth superimposed upon historical climate variability results in only a very small probability of annual reservoir depletion through 2057. In contrast, a scenario of 20 percent reduction in the annual Colorado River flow due to climate change by 2057 results in a near 10-fold increase in the probability of annual reservoir depletion by 2057, to about 50 percent. However, their analysis also shows that alterations to current management policies (e.g., reducing deliveries more often) could mitigate some of the increased risk due to climate change-induced reductions in flows.

Subsequently, Barnett and Pierce (2009) improved their earlier model in light of the Barsugli et al. (2009) criticisms, and found results similar to those of Barsugli et al. (2009) and Rajagopalan et al. (2009). They indicate that under a climate-change-induced 10 percent reduction flows by 2060, mean annual delivery shortfalls will be about one MAF, increasing to two MAF under a 20 percent flow reduction.

In all of these studies, streamflow in the LCRB is not fully represented; the non-Gila flows in the LCRB are simulated as a constant term, and inflows from the Gila River are not included at all. The Gila River is ephemeral under current management, but during wet years it has substantial inflows to the Colorado that can potentially be used to meet the US delivery obligation to Mexico. Thus our contention is that a better representation of LCRB flows in the system model would allow a more robust depiction of both water supply risk and the management options for mitigating that risk.

2.7.2 Methods

The system response analysis was performed using a water-balance model that is simple yet reasonably representative of the water resources system in the basin (Figure 20). The model was previously used in Rajagopalan et al. (2009) to investigate the risk of active system storage being depleted under different scenarios. For this project, the model setup added variability in LCRB flow and the ability of periodic Gila River discharges to reduce the releases needed from reservoir storage to meet the Mexico delivery obligations. As in Rajagopalan et al. (2009), the water-balance model was driven by natural variability alone and with climate change scenarios (progressive flow reductions), under two different reservoir operation rules and demand management alternatives.

Figure 20. Schematic of the water-balance model used for the system response analysis, modified from Rajagopalan et al. (2009) to include the Gila River inflows. The "bathtub" represents the aggregate CRB reservoir storage capacity of 60 MAF.

The core of the water-balance model is this equation:

$$S_t = S_{t-1} + I_{UB,LB} - O_{UB} - TL*O_{LB} - TL*(O_{MX} - I_{Gila}) - E$$

- S_t is storage at current time step (year)
- S_{t-1} storage at previous time step
- $I_{UB,LB}$ is inflow from Upper Basin (UB) and Lower Basin (LB)
- O_{UB} is outflow (releases) to meet UB demand
- O_{LB} is outflow (releases) to meet LB demand
- O_{MX} is outflow (releases) to meet Mexico delivery obligation of 1.5 MAF
- I_{Gila} is the inflow from the Gila River, capped at 1.5 MAF
- TL is transmission losses, equal to 11.5 percent
- E is evaporation, a function of reservoir storage

UCRB inflows: Tree-ring reconstructed Lees Ferry streamflows from Woodhouse et al. (2006) and Meko et al. (2007) were emulated using a non-homogenous Markov Chain model on the paleoflows, combined with K-nearest neighbor resampling of the observed flows, as in Prairie et al. (2008). In this approach, the hydrologic state (wet or dry) is generated based on the non-homogeneous Markov chain model fitted to the paleo-reconstructed data. Then a streamflow magnitude (e.g., 13.821 MAF) is resampled from the observed record, with the resampling conditioned on the hydrologic state and the previous year's flow.

LCRB (non-Gila) inflows: The Local Poly tree-ring reconstruction of the flows at the five good LCRB CRSS nodes, described earlier in this report, was used as the basis for this term. The reconstructed values were resampled, conditioned on the simulated Lees Ferry flow to capture the relationship (r = 0.54) between LCRB flows and Lees Ferry flows. To represent the contribution of the four noise nodes, a value was randomly selected from a distribution with a mean of 0.50 MAF, the mean of the four noise nodes.

Gila River inflows: The Extreme Value Analysis (EVT) Peaks-over-Threshold (POT) tree-ring reconstruction (1612–2005) of the gaged Gila River flows near Dome, AZ flows, described earlier in this report, was used as the basis of this term, as follows:

(1) We randomly selected a 50-year period from the streamflow reconstruction.

(2) For each year in the 50-year period, a random number between zero and one was simulated and compared against the exceedance probability obtained from the logistic regression for the corresponding year. If the random number was less than the exceedance probabilities, then an exceedance occurred. Otherwise, the year was a non-exceedance.
(3) For all the exceedance years, a magnitude was generated from the GPD. The scale parameter was estimated from the nonstationary model and a random value is generated from the GPD using the estimated scale parameter.
(4) This was repeated for the 10,000 simulations.

Evaporation was calculated as a function of reservoir storage, as in Rajagopalan et al. (2009). As storage decreases, so does the reservoir surface area, as documented in Reclamation (2007), Appendix A. Evaporation was calculated by multiplying surface area by the average annual evaporation coefficient.

Four management scenarios (Alternatives A–D; Table 2) were evaluated, representing two different policies for mandated delivery shortages to the LCRB, and two different UCRB demand schedules (Table 3). The first delivery shortage policy was based on the Interim Guidelines found in the 2007 Environmental Impact Statement (EIS) (Reclamation, 2007). The second was a more aggressive option that mandates smaller delivery shortages to be enacted sooner than the Interim Guidelines call for. These options were the same as those considered in Rajagopalan et al., 2009. Two scenarios for future increases in UCRB demand were considered. Under Alternatives A and B, the demand schedule from Reclamation (2007), Appendix N, is used. Under Alternatives C and D, the initial demand is reduced to the actual levels seen in 2008 (a reduction of 0.843 MAF), but the same yearly increase as found in the Reclamation (2007) demand schedule is then applied. In all four scenarios, deliveries to the LCRB were set at 7.5 MAF plus transmission losses of 11.5 percent. Deliveries to Mexico are set at 1.5 MAF minus contributions from the Gila River plus transmission losses on any remaining amount. The transmission losses account for evaporation from Lake Mohave and Lake Havasu, riparian corridor transpiration, and other operational losses (Rajagopalan et al. 2009). These transmission losses are roughly consistent with the estimate from Reclamation (1946) of channel losses under natural conditions of 1.18 MAF (about six percent) below Lake Mead.

Table 2. The four management alternatives (A–D) considered in the system response modeling, and the demand schedule and delivery shortage policy used for each.

Alternative	Demand Schedule	Delivery Shortage Policy	Initial Storage (MAF)
A	EIS	Interim Guidelines	30
B	EIS	Aggressive	30
C	Modified EIS	Interim Guidelines	30
D	Modified EIS	Aggressive	30

Table 3. The cuts to LCRB deliveries mandated at specified reservoir levels under the Interim Guidelines (left) and the Aggressive Shortage Policy (right).

Interim Guidelines		**Aggressive Shortage Policy**	
Reservoir Level	**Delivery Cut**	**Reservoir Level**	**Delivery Cut**
36%	0.333 MAF	50%	5% (0.375 MAF)
30%	0.417 MAF	40%	6% (0.450 MAF)
23%	0.500 MAF	30%	7% (0.525 MAF)
		20%	8% (0.600 MAF)

Three climate scenarios were considered. The first is natural climate variability based on historical and paleo variability, the second is a 10 percent reduction in the mean streamflow over a 50-year period, and the third is a 20 percent reduction. For the flow reductions, a linear decreasing trend was applied so that no change was felt in the first year of the simulation and the full decrease was felt by the final year. For both climate change scenarios, the same reductions were applied to both UCRB and LCRB flows.

The water-balance model was then run for 10,000 50-year simulations on a yearly time step. For comparison, the model was also run without the Gila River inflow component (thus similar to Rajagopalan et al., 2009). A suite of variables were computed from the set of runs, for each scenario: (1) the probability of storage going dry in any given year, (2) average shortage magnitude per year in a 50-year period, and (3) the number of shortages in a 50-year period.

2.7.3 Results

The probability (or risk) of total storage in the water-balance model going dry in each year based on the streamflow simulations, climate scenarios, and management alternatives are shown in Figures 21 and 22. For comparison we also show the results without including Gila River inflows, which are similar to those in Rajagopalan et al. (2009). An important caveat is that the modeling assumed that 100 percent of the Gila River inflows (up to 1.5 MAF/year, the delivery obligation to Mexico) can be used to reduce Lake Mead releases. In practice, due to flow timing and water quality issues, the substitution achieved has been much less than 100 percent. But the modeling result points to the potential for more deliberate management of Gila inflows to reduce system risk.

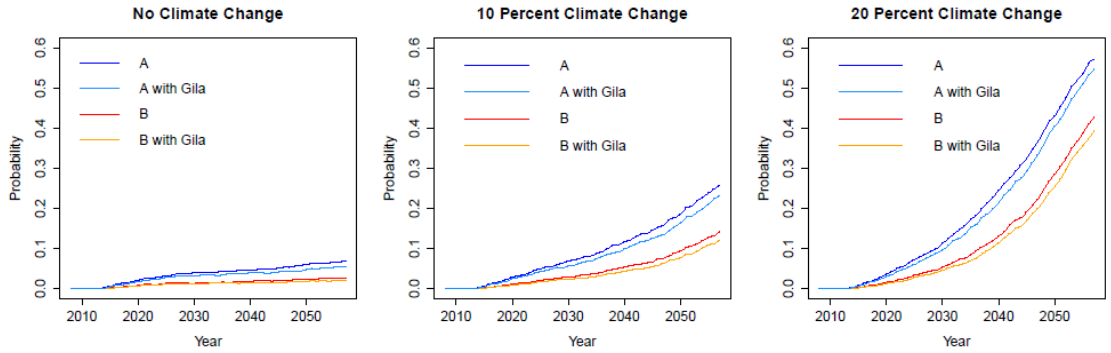

Figure 21: Risk of drying (depleting all reservoir storage in a given year) for Alternatives A and B. Including the Gila River into the water-balance model decreases the risk of drying for all climate change scenarios. (left) No climate change induced flow reductions. (center) 10 percent climate change induced flow reduction by 2057. (right) 20 percent climate change induced flow reduction by 2057.

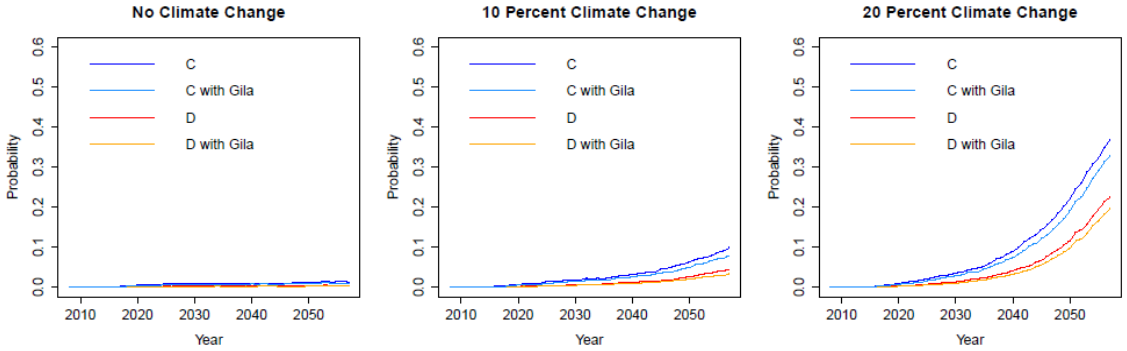

Figure 22: Risk of drying (depleting all reservoir storage in a given year) for Alternatives C and D. Same climate scenarios as in previous figure.

Under natural climate variability alone, the risk of drying up storage is very low (Figure 3.8), less than seven percent for the entire period, under all management scenarios. This is reduced by including Gila River inflows and further reduced when combined with more aggressive management (Figure 3.9). Under a 20 percent reduction in flow by 2057 due to climate change, the risk of drying under management alternative A is 51.4 percent, but 49.5 percent when the inflows from the Gila River are included. Similar mitigation of risk occurs with the inclusion of the Gila River under the other alternatives. For example, in alternative C, the risk of drying by 2057 is 35.4 percent without the Gila River inflows and it reduced to 32.7 percent, with Gila inflows, about an eight percent decrease in risk. Similar risk profiles are seen with a 10 percent reduction.

Boxplots of average shortage per year in a 50-year period are shown in Figures 23 and 24. Shortages occur due to the rule-mandated cut backs in delivery as reservoir storage drops or due to the system's physical inability to meet the full demands. One consistent feature across all the boxplots is the highly skewed nature of the distribution of delivery shortages. Incorporating the Gila reduces the both magnitude of shortage and, more importantly, the variability in the shortage.

With current operations (alternative A), the shortages tend to be large. With a more aggressive supply management, where small delivery cuts are made as the reservoir levels fall, the shortages are smaller. Including the Gila River further reduces shortage magnitude. The Gila River, even with its intermittency, can contribute meaningfully to the Colorado River system water supply.

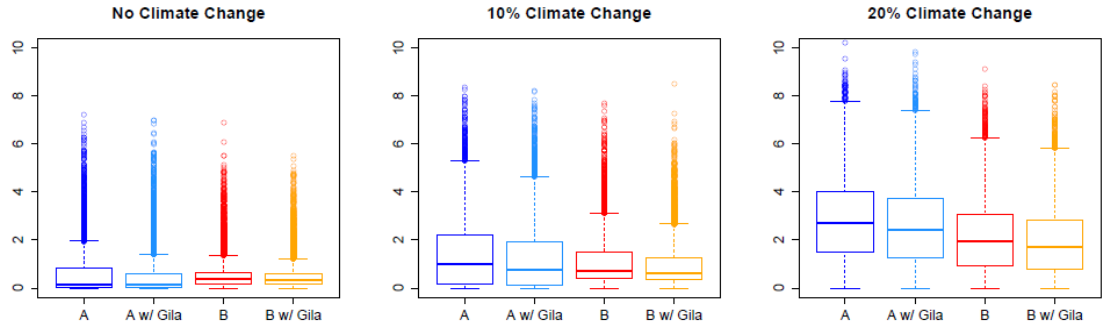

Figure 23: Boxplots showing the average delivery shortage volume in a 50-year period for alternatives A and B. (a) Natural variability only, no climate change induced flow reductions. (b) 10 percent climate change induced flow reduction. (c) 20 percent climate change induced flow reduction.

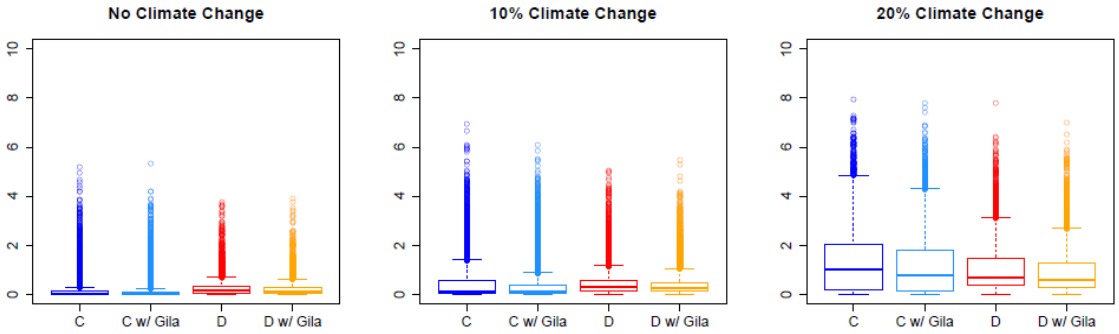

Figure 24: Boxplots showing the average delivery shortage volume in a 50-year period for alternatives C and D. (a) Natural variability only, no climate change induced flow reductions. (b) 10 percent climate change induced flow reduction. (c) 20 percent climate change induced flow reduction.

Boxplots of the number of shortages in a 50-year period are shown in Figures 25 and 26. Under the Interim Guideline operations (alternatives A and C), including Gila flows provides a source of relief that reduces the number of shortages. For the aggressive shortage policy alternatives (B and D), the number of shortages is higher. This is expected because these alternatives impose shortages sooner relative to current operations, but the average magnitude of shortages is smaller. An aggressive reservoir management policy does force users to deal with more frequent shortages; however they are of a smaller magnitude. Dealing with small shortages more frequently has a large, positive impact on overall system risk. The aggressive management policy reduces risk levels under a 20 percent climate change from 50 percent in Alternative A to 38 percent in Alternative B (including Gila inflows), as seen in Figure 21.

Demand management also has large impacts on system risk. Comparing Alternative A with Alternative C at 20 percent climate change drops the risk from 50 percent to 33 percent (Figures

21 and 22). This is an even larger reduction in risk than was achieved under the aggressive shortage policy.

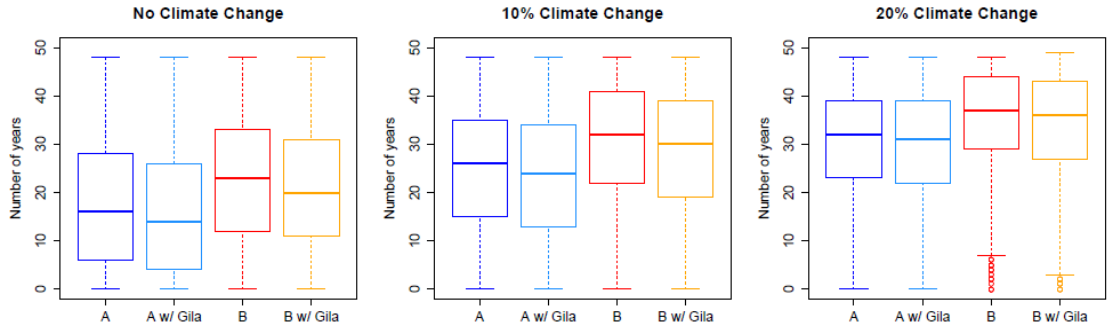

Figure 25: Boxplots showing the number of years with a delivery shortage in a 50-year period for alternatives A and B. (a) Natural variability only, no climate change induced flow reductions. (b) 10 percent climate change induced flow reduction. (c) 20 percent climate change induced flow reduction.

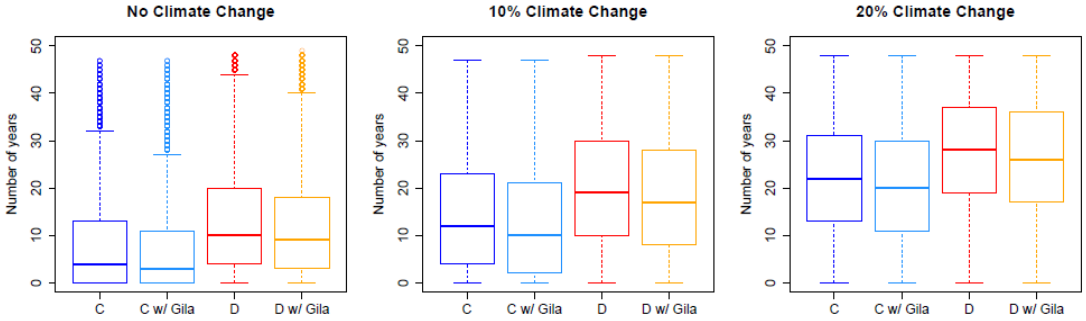

Figure 26: Boxplots showing the number of years with a delivery shortage in a 50-year period for alternatives C and D. (a) Natural variability only, no climate change induced flow reductions. (b) 10 percent climate change induced flow reduction. (c) 20 percent climate change induced flow reduction.

Different climate change reductions on Gila River do not seem to substantially impact the Gila's beneficial effect overall drying risk (Figures 21 and 22). By computing the total volume of Gila River contributions in a 50-year period (shown as boxplots in Figure 27), we see the contribution range decreases with climate-change-induced flow reductions but the median remains the same. This is due to the 1.5 MAF cap on allowable contributions from the Gila River. Also, the Gila is modeled by a POT process so there is either a large amount of flow, or there is no flow, thus, even a 20 percent reduction of the extremely high flow years does not drop the flows below the 1.5 MAF cap.

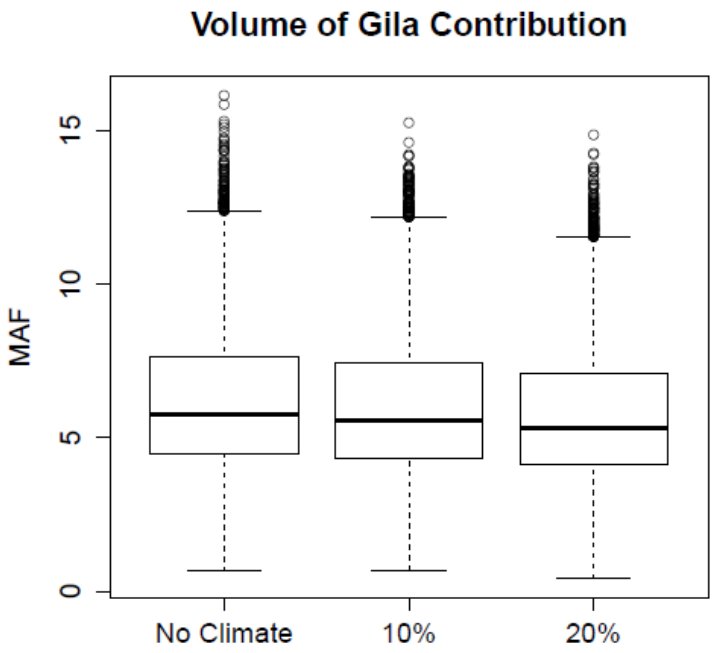

Figure 27: Boxplots showing the showing the total volume of flow from the Gila River in a 50-year period under the three climate change scenarios (a) Natural climate Variability only; (b) 10 percent climate change induced reduction of flow; (c) 20 percent climate change induced reduction of flow.

Even though the Gila River inflows are intermittent under current management and can only contribute to CRB water supplies by helping to meet the 1.5 MAF delivery obligation to Mexico, they still has a positive impact on system reliability, reducing the frequency and the magnitude of delivery shortages for all of the simulations. The system risk responded consistently to the addition of periodic inflows from the Gila, though is much more sensitive to the choice of demand schedule, climate change, and management policy.

3. Conclusions

Overall, the project was successful in its objectives of (1) reconstructing the long-term hydrologic variability of the LCRB using multiple statistical methods, including two novel approaches, and (2) incorporating that variability into Colorado River Basin system risk modeling. We deployed two new reconstruction methods, one of which has for the first time allowed paleo-reconstruction of the highly intermittent gaged flows of the Gila River. We found that the variability of LCRB flows does matter to system risk, and that in particular the Gila River can have a measurable impact on system risk due to its periodic and significant discharges into the mainstem.

During the course of the research, we also found that the naturalized intervening flows on the Colorado River between Lees Ferry and Imperial Dam used in previous studies of Colorado River system risk are problematic and likely overestimate the actual inflows below Lake Mead. The reconstructions of flows on this reach were probably degraded because of the uncertainties in

these flows. The estimates for the natural flows for the Gila River, based on Reclamation (1946) might also be improved, or at least confirmed with modern hydrologic modeling. A secondary objective of the project was to estimate a total natural flow for the Colorado River at the Northerly International Boundary (NIB) near Yuma for each year of the paleo period (~1600 onward) by summing the reconstructed flows for (1) Lees Ferry, (2) the Gila near Dome, and (3) the mainstem between Lees Ferry and Imperial Dam, respectively. However, the third component in that list had greater uncertainties than we had hoped, and we found that a fourth component needs further refinement: the substantial channel losses under natural conditions below Lake Mead.

Potential future work would be fruitfully focused on one or both of two tracks. The first would be to improve the estimates of natural inflows for both the Gila and the LCRB mainstem, and the channel losses below Mead, to close the total budget for the natural flows of the Colorado River Basin. The second track would be to investigate the feasibility of actively managing Gila River inflows for risk reduction, starting with assessment of the recent "substitution efficiency" of Gila inflows in supplanting Lake Mead releases to satisfy the Mexico delivery obligation, and then identifying ways to increase that efficiency.

4. References

Apipattanavis, S., Rajagopalan, B., and Lall, U. (2010). Local polynomial-based flood frequency estimator for mixed population. *Journal of Hydrologic Engineering*, 15(9):680-691.

Barnett, T. and D. Pierce (2008). When will Lake Mead go dry? *Water Resources Research* 44.

Barnett, T. and Pierce, D. (2009). Sustainable water deliveries from the Colorado River in a changing climate. *Proceedings of the National Academy of Sciences*, 106(18).

Barsugli, J., K. Nowak, B. Rajagopalan, J. Prairie, and B. Harding (2009). Comment on "When will Lake Mead go dry?" by T.P. Barnett and D.W. Pierce. *Water Resources Research* 45.

Bracken, C., Rajagopalan, B., and Prairie, J. (2010). A multi-site seasonal ensemble streamflow forecasting technique. *Water Resources Research*.

Christensen, N. and Lettenmaier, D. (2007). A multimodel ensemble approach to assessment of climate change impacts on the hydrology and water resources of the Colorado River Basin. *Hydrology and Earth System Sciences*, 11:1417-1434.

Coles, S. (2001). *An Introduction to Statistical Modeling of Extreme Values.* Volume 208. Springer Series of Statistics.

Cook, E. and Kairiukstis, L. (1990). *Methods of Dendrochronology: Application in the Environmental Sciences.* Kluwer Academic Publishers.

Everitt, B., Landau, S., and Leese, M. (2001). *Cluster analysis.* A. O. Arnold.

Gangopadhyay, S. (2012). Personal communication, February 24, 2012.

Gangopadhyay, S., Harding, B., Rajagopalan, B., Lukas, J., and Fulp, T. (2009). A non-parametric approach for paleohydrologic reconstruction of annual streamflow ensembles. *Water Resources Research* 45, W06417.

Grantz, K. and Rajagopalan, B. (2005). A technique for incorporating large-scale climate information in basin-scale ensemble streamflow forecasts. *Water Resources Research*, 41.

Gray, S. T., Lukas, J. J., and Woodhouse, C. A. (2011). Millennial-length records of streamflow from three major Upper Colorado River tributaries. *Journal of the American Water Resources Association*, 47(4):702-712.

Griffin, D., Meko, D.M., Touchan, R., Leavitt, S.W., and C.A. Woodhouse. (2011) Latewood chronology development for summer moisture reconstruction in the U.S. Southwest. *Tree-Ring Research* 67:87-101.

Fritts, H. C. (1976). *Tree Rings and Climate*. Academic Press, New York.

Hidalgo, H. G., Piechota, T. C., and Dracup, J. A. (2000). Alternative principal components regression

procedures for dendrohydrologic reconstructions. *Water Resources Research*, 36(11):3241-3249.

Katz, R. W., M. B. Parlange, and P. Naveau (2002). Statistics of extremes in hydrology. *Advances in Water Resources* 25, 1287-1304.

Lall, U. and Sharma, A. (1996). A nearest-neighbor bootstrap for resampling hydrologic time series. *Water Resources Research*, 32(3):679-693.

McCullagh, P. and Nelder, J. (1989). *Generalized Linear Models.* Chapman and Hall, London.

Meko, D. and Graybill, D. A. (1995). Tree-ring reconstruction of upper Gila River discharge. *Water Resources Bulletin*, 31(4):605-616.

Meko, D. and Woodhouse, C. (2011). Application of streamflow reconstruction to water resource management. In Hughes, Swetnam, and Diaz, editors, *Dendroclimatology: Progress and Prospects*. Springer, New York.

Meko, D., Woodhouse, C., Baisan, C. A., Knight, T., Lukas, J. J., Hughes, M. K., and Salzer, M. W. (2007). Medieval drought in the Upper Colorado River Basin. *Geophysical Research Letters*, 34.

Meko, D. M. and Hirschboeck, K. K. (2008). The current drought in context: A tree-ring based evaluation of water supply variability for the Salt-Verde river basin. Technical report, The University of Arizona's Laboratory of Tree-Ring Research and The Salt River Project.

Milly, P. C. D., Dunne, K. A., and Vecchia, A. V. (2005). Global pattern of trends in streamflow and water availability in a changing climate, Nature, 438, 347–350.

Prairie, J., Rajagopalan, B., Fulp, T., and Zagona, E. (2006). Modified K-NN model for stochastic streamflow simulation. *Journal of Hydrologic Engineering*, 11(4).

Prairie, J., K. Nowak, B. Rajagopalan, U. Lall, and T. Fulp (2008). A stochastic nonparametric approach for streamow generation combining observational and paleoreconstructed data. *Water Resources Research* 44.

Rajagopalan, B. and U. Lall (1999). A K-nearest neighbor simulator for daily precipitation and other weather variables. *Water Resources Research*, 35(10):3089-3101.

Rajagopalan, B., Nowak, K., Prairie, J., Hoerling, M., Harding, B., Barsugli, J., Ray, A., and Udall, B. (2009). Water Supply Risk on the Colorado River: Can Management Mitigate? *Water Resources Research* 45, W08201, doi:10.1029/2008WR00765.

Reclamation (1946). The Colorado River: A comprehensive report of the development of the water resources of the Colorado River Basin for irrigation, power production, and other beneficial uses in Arizona, California, Nevada, New Mexico, Utah, and Wyoming. Bureau of Reclamation Project Planning Report 34-8-2, United States Department of Interior, Washington: Government Printing Office.

Reclamation (2007). Final environmental impact statement: Colorado River interim guidelines

for LCRB shortages and coordinated operations for Lakes Powell and Mead. Technical report, United States Department of Interior, Boulder City, Nevada.

Reclamation (2011a). Colorado River Basin Water Supply and Demand Study, Interim Report No. 1, Technical Report B – Water Supply Assessment, Bureau of Reclamation, US Department of the Interior.

Reclamation (2011b). West-Wide Climate Risk Assessments: Bias-Corrected and Spatially Downscaled Surface Water Projections, Bureau of Reclamation, US Department of the Interior.

Regonda, S. K., Rajagopalan, B., Clark, M., and Zagona, E. (2006). A multimodel ensemble forecast framework: Application to spring seasonal flows in the Gunnison River basin. *Water Resources Research*, 42.

Smith, L.P., and Stockton, C.W. (1981). Reconstructed streamflow for the Salt and Verde Rivers from tree-ring data. *Water Resources Bulletin*, v. 17, no. 6, p. 939-947.

Stockton, C. and Jacoby, G. (1976). Long-term surface-water supply and streamflow trends in the Upper Colorado River Basin based on tree-ring analysis. Lake Powell Research Project Bulletin, 18.

Towler, E., Rajagopalan, B., and Gilleland, E. (2010a). Modeling hydrologic and water quality extremes in a changing climate: A statistical approach based on extreme value theory. *Water Resources Research*, 46.

Towler, E., Rajagopalan, B., and Summers, R. S. (2010b). An approach for probabilistic forecasting of seasonal turbidity threshold exceedance. *Water Resources Research*, 46.

Wade, L. (2012). Paleohydrology reconstructions for the lower Colorado River Basin and implications for water supply reliability. Master's thesis, University of Colorado.

Woodhouse, C. A., Gray, S. T., and Meko, D. M. (2006). Updated streamflow reconstructions for the Upper Colorado River Basin. *Water Resources Research*, 42(5):16.

Woodhouse, C. A. and Lukas, J. J. (2006). Multi-century tree-ring reconstructions of Colorado streamflow for water resource planning. *Climatic Change*, 78(2-4):293-315.